

AD-A118 425

AIR FORCE ENVIRONMENTAL TECHNICAL APPLICATIONS CENTER--ETC F/G 4/2
A COMPARISON OF THE AFGL FLASH, DRAPER DART AND AWS HAZE MODELS--ETC(U)
MAR 82 P J BREITLING

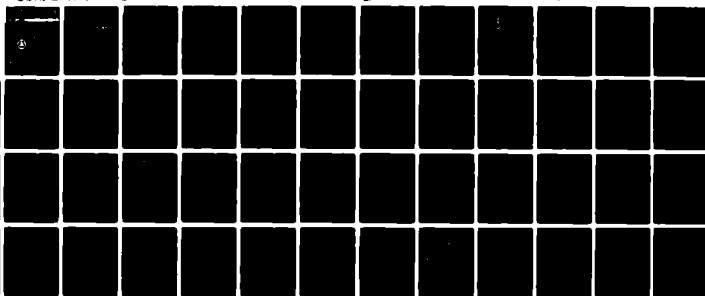
UNCLASSIFIED

USAFETAC/TN-82/001

SBI-AD-E850 180

NL

171
AF-425



END

03-02
DTIC

AOE 850 180
USAFETAC/TN-82/001



AD A118425



A COMPARISON OF THE AFGL FLASH,
DRAPER DART AND AWS HAZE MODELS WITH
THE RAND WETTA MODEL FOR CALCULATING
ATMOSPHERIC CONTRAST REDUCTION

BY

DR. PATRICK J. BREITLING

MARCH 1982

Approved For Public Release; Distribution Unlimited

UNITED STATES AIR FORCE
AIR WEATHER SERVICE (MAC)
USAF
ENVIRONMENTAL
TECHNICAL APPLICATIONS
CENTER

SCOTT AIR FORCE BASE, ILLINOIS 62225



82 07 27 072

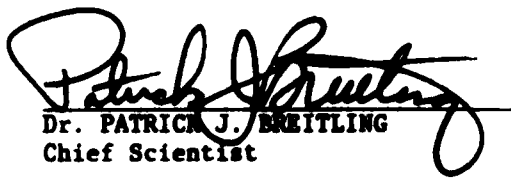
DMC FILE COPY

REVIEW AND APPROVAL STATEMENT

USAFETAC/TN-82/001, A COMPARISON OF THE AFGL FLASH, DRAPER DART AND AWS HAZE MODELS WITH THE RAND WETTA MODEL FOR CALCULATING ATMOSPHERIC CONTRAST REDUCTION, March 1982, is approved for public release. There is no objection to unlimited distribution of this document to the public at large, or by the Defense Technical Information Center (DTIC) to the National Technical Information Service (NTIS).

This Technical Note has been reviewed and is approved for publication.


PETER J. HAVANAC, LtCol, USAF
Chief, Aerospace Sciences Branch
Reviewing Officer


Dr. PATRICK J. BREITLING
Chief Scientist

FOR THE COMMANDER


WALTER S. BURGMANN
Scientific and Technical Information
Officer (STINFO)
19 APR 1992

~~UNCLASSIFIED~~
SECURITY CLASSIFICATION OF THIS PAGE (When Data Entered)

REPORT DOCUMENTATION PAGE		READ INSTRUCTIONS BEFORE COMPLETING FORM
1. REPORT NUMBER USAFETAC/TN-82/001	2. GOVT ACCESSION NO. <i>AD-A118 425</i>	3. RECIPIENT'S CATALOG NUMBER
4. TITLE (and Subtitle) A COMPARISON OF THE AFGL FLASH, DRAPER DART AND AWS HAZE MODELS WITH THE RAND WETTA MODEL FOR CALCULATING ATMOSPHERIC CONTRAST REDUCTION	5. TYPE OF REPORT & PERIOD COVERED Technical Note	
7. AUTHOR(s) Patrick J. Breitling	6. PERFORMING ORG. REPORT NUMBER	
9. PERFORMING ORGANIZATION NAME AND ADDRESS US Air Force Environmental Technical Applications Center/DN Scott AFB IL 62225	10. PROGRAM ELEMENT, PROJECT, TASK AREA & WORK UNIT NUMBERS	
11. CONTROLLING OFFICE NAME AND ADDRESS US Air Force Environmental Technical Applications Center Scott AFB IL 62225	12. REPORT DATE March 1982	
14. MONITORING AGENCY NAME & ADDRESS (if different from Controlling Office)	13. NUMBER OF PAGES 55	
	15. SECURITY CLASS. (of this report) UNCLASSIFIED	
	15a. DECLASSIFICATION/DOWNGRADING SCHEDULE	
16. DISTRIBUTION STATEMENT (of this Report) Approved for public release; distribution unlimited		
17. DISTRIBUTION STATEMENT (of the abstract entered in Block 20, if different from Report)		
18. SUPPLEMENTARY NOTES A paper by the same title as this report was presented by the author at the 8th Technical Exchange Conference, Air Force Academy, Colorado, 28 November-1 December 1978.		
19. KEY WORDS (Continue on reverse side if necessary and identify by block number) Atmospheric models, radiative transfer models, contrast reduction, contrast transmittance, precision guided munitions, atmospheric transmission, television-guided munitions, precision guidance, AWS Haze Model, Draper Lab DART model, RAND Corp. WETTA model, Monte Carlo model		
20. ABSTRACT (Continue on reverse side if necessary and identify by block number) In 1975 the US Air Force Environmental Technical Applications Center (USAFETAC) was tasked to develop a model to calculate the lock-on range for TV-guided precision guided munitions. Investigation revealed the availability of several models for calculating contrast reduction by the atmosphere. These models, the Air Force Geophysics Lab (AFGL) FLASH model, the Air Weather Service (AWS) Haze Model, the Draper Lab DART model, and the RAND Corp. WETTA model, were compared with one another using the same input data. The FLASH Monte Carlo model was assumed as the standard for the comparison. Visible		

Block 20 continued:

contrast transmission values were computed for all models for a TV sensor at 12,000 feet AGL, for two mixing depths (200 and 1500 meters), two visibilities (5 and 23 kilometers), three solar zenith angles (20, 60, and 85 degrees), three albedos (.06, .18, and .80), and seven dive angles (85, 70, 50, 30, 20, 10 and 7 degrees). If one accounts for the difference in optical depths which results from Huschke's (RAND Corp.) stair step treatment of vertical extinction coefficients, his model does an acceptable job of approximating FLASH contrast transmission values for a visibility of 23 kilometers. When the visibility is 5 kilometers, the agreement is not as good due to a combination of mathematical and geometrical factors.

Accession For	
NTIS GRA&I <input checked="" type="checkbox"/>	
DTIC TAB <input type="checkbox"/>	
Unannounced <input type="checkbox"/>	
Justification	
By	
Distribution/	
Availability Codes	
Dist	Avail and/or Special
A	



UNCLASSIFIED

CONTENTS

	Page
Chapter 1 Introduction	1
Chapter 2 Background Information	2
Chapter 3 Contrast Transmittance Comparison for 23 Km.	9
Chapter 4 Contrast Transmittance Comparison for a 5-Km Surface Visibility	31
Chapter 5 Conclusions and Recommendations	49
REFERENCES	51
GLOSSARY	52

ILLUSTRATIONS

Figure 1 Horizontal Visibility Profiles for Stair-Step and Exponential Extinction Coefficient	4
Figure 2 Comparison of Contrast Transmittance Integrated over Eight Wavelength Intervals with the Contrast Transmittance for 0.55 Microns.	6
Figure 3 Variation of Contrast Transmittance with Azimuth Angle for FLASH Model.	7
Figure 4 Contrast Transmittance at 20 Degrees Solar Zenith, Albedo of 0.18, and 23-km Surface Visibility	10
Figure 5 Contrast Transmittance at 60 Degrees Solar Zenith, Albedo of 0.18, and 23-km Surface Visibility	11
Figure 6 Contrast Transmittance at 85 Degrees Solar Zenith, Albedo of 0.18, and 23-km Surface Visibility	12
Figure 7a Model Comparisons at 20 Degrees Solar Zenith, Albedo of 0.18, and 23-km Surface Visibility	13
Figure 7b Model Comparisons at 20 Degrees Solar Zenith, Albedo of 0.18, and 23-km Surface Visibility	14
Figure 8 Contrast Transmittance at 20 Degrees Solar Zenith, Albedo of 0.06, and 23-km Surface Visibility	15
Figure 9 Contrast Transmittance at 60 Degrees Solar Zenith, Albedo of 0.06, and 23-km Surface Visibility	16
Figure 10 Contrast Transmittance at 85 Degrees Solar Zenith, Albedo of 0.06, and 23-km Surface Visibility	17
Figure 11 Contrast Transmittance at 20 Degrees Solar Zenith, Albedo of 0.80, and 23-km Surface Visibility	19
Figure 12 Contrast Transmittance at 60 Degrees Solar Zenith, Albedo of 0.80, and 23-km Surface Visibility	20
Figure 13 Contrast Transmittance at 85 Degrees Solar Zenith, Albedo of 0.80, and 23-km Surface Visibility	21
Figure 14a Model Comparison at 60 Degrees Solar Zenith, Albedo of 0.18, and 23-km Surface Visibility	22
Figure 14b Model Comparison at 60 Degrees Solar Zenith, Albedo of 0.18, and 23-km Surface Visibility	23
Figure 15a Model Comparisons at 85 Degrees Solar Zenith, Albedo of 0.18, and 23-km Surface Visibility	24
Figure 15b Model Comparisons at 85 Degrees Solar Zenith, Albedo of 0.18, and 23-km Surface Visibility	25
Figure 16 RMSE Model Comparisons for Albedo of 0.18 and 23-km Surface Visibility	26
Figure 17 RMSE for All Solar Zenith Angles Versus RMSE without 85- and 70-Degree Solar Zenith Angles	27
Figure 18 Total Optical Depth Below 12,000-Ft Viewing Altitude for 23-km Surface Visibility	28
Figure 19 Contrast Transmittance at 20 Degrees Solar Zenith, Albedo of 0.06, and 5-km Surface Visibility	32
Figure 20 Contrast Transmittance at 20 Degrees Solar Zenith, Albedo of 0.18, and 5-km Surface Visibility	33
Figure 21 Contrast Transmittance at 20 Degrees Solar Zenith, Albedo of 0.80, and 5-km Surface Visibility	34
Figure 22 Model Comparisons at 20 Degrees Solar Zenith and 5-km Surface Visibility	35

Figure 23	Contrast Transmittance at 60 Degrees Solar Zenith, Albedo of 0.06, and 5-km Surface Visibility.	36
Figure 24	Contrast Transmittance at 60 Degrees Solar Zenith, Albedo of 0.18, and 5-km Surface Visibility.	37
Figure 25	Contrast Transmittance at 60 Degrees Solar Zenith, Albedo of 0.80, and 5-km Surface Visibility.	38
Figure 26	Model Comparisons at 60 Degrees Solar Zenith and 5-km Surface Visibility.	39
Figure 27	Contrast Transmittance at 85 Degrees Solar Zenith, Albedo of 0.06, and 5-km Surface Visibility.	40
Figure 28	Contrast Transmittance at 85 Degrees Solar Zenith, Albedo of 0.18, and 5-km Surface Visibility.	41
Figure 29	Contrast Transmittance at 85 Degrees Solar Zenith, Albedo of 0.80, and 5-km Surface Visibility.	42
Figure 30	Model Comparisons at 85 Degrees Solar Zenith, Albedo of 0.18, and 5-km Surface Visibility.	43
Figure 31	Model Comparisons at 85 Degrees Solar Zenith, Albedo of 0.80, and 5-km Surface Visibility.	44
Figure 32	RMSE Model Comparisons for Albedo of 0.18 and 5-km Surface Visibility.	45
Figure 33	Total Optical Depth Below 12,000-Ft Viewing Altitude for 5-km Surface Visibility	47

Chapter 1

INTRODUCTION

"Smart Bombs" or, more properly, Precision Guided Munitions (PGMs) were first introduced during the war in Southeast Asia. Both the Electro-Optical Guided Bomb (EOGB) and the Laser Guided Bomb (LGB) were much more successful at destroying enemy targets than conventional unguided iron bombs. Since then, numerous other PGMs have been designed, developed, and deployed, each employing a particular segment of the electromagnetic spectrum for guidance. Because successful use of these weapons depends on a wide variety of atmospheric variables (i.e., clouds, haze, illumination level, etc.), Air Weather Service (AWS) had to develop new weather-support techniques for these weapons.

This report deals with weather support to a particular kind of PGM, namely, those that employ a TV sensor mounted in the nose of the weapon. Specifically, what follows is an evaluation of the largely statistical techniques developed by Mr Ralph Huschke of RAND Corporation (Huschke, 1976). While the Huschke method "permits the direct evaluation of weapons system performance in any weather situation or climatic regime that can be extracted as a subset of the weather data base," it is not designed specifically as an operational weather support technique. Rather, it is intended as a method which will test the use of a statistical "best fit" between the sky-ground ratio and available weather data to infer contrast transmittance. Thus, the method is only as good as the relationships that Huschke gives in his report (Huschke, 1976, page 11), i.e., its ability to duplicate what goes on in the real world. Its operational weather support utility as a forecast tool is yet to be proven. The reader should be thoroughly familiar with the techniques described in Huschke's report prior to reading what follows.

Chapter 2

BACKGROUND INFORMATION

To successfully support TV-guided PGM operations, one must employ far more sophisticated techniques than those commonly used in conventional aviation meteorology. Ambient and predicted future illumination levels, target-to-background contrast levels, and the temporal and spatial variability of atmospheric haze are a few of the factors which contribute to PGM guidance and are not a part of routine aviation weather support. A complete discussion of the complexities of such specialized support is available in the AWS Electro-Optical (EO) Handbook (Cottrell, et.al., 1979) and will not be repeated here.

The AWS TV-Guided Maverick Missile Weather Support Plan (WSP) tasks the USAF Environmental Technical Applications Center (USAFETAC) to "Provide Phase I technique development to produce the appropriate forecast methods and determine the forecast skill levels." Since the adoption of this WSP and with the support of the EO Systems Working Group (SWG) USAFETAC has culled, from the scientific literature, a variety of atmospheric models which were designed to simulate the loss of visible light contrast between a ground target and an airborne TV sensor. These models fall into two general categories: radiative transfer models which employ rigorous scattering theory to compute contrast loss for specified geometrical and environmental conditions and the empirical, so-called "cookbook," models or techniques which employ grosser assumptions than the above theoretical models and often involve manual methods. Examples of the first category are the Air Force Geophysics Laboratory's (AFGL) FLASH Model (Collins and Blattner, 1970), the Draper Lab's DART Model (Whitney and Malchow, 1977), and the AWS Haze Model (Breitling and Pilipowskyj, 1970). Examples of the faster empirical techniques are those due to Huschke (1976), the AWS EO Handbook (Cottrell, et.al., 1979), and the 5th Weather Wing Manual Weather Support Procedures (5WW, 1977).

Each model or technique has obvious advantages and drawbacks. The FLASH Model offers a rigorous and exact treatment of the radiative transfer process, but could not be used to support PGM operations in anything approaching real time because it requires enormous amounts of computer time. The DART Model is some 30 times faster, but is still too slow. The AWS Haze Model is computationally fast, but some of its restrictive assumptions (flat earth, no multiple scattering, etc.), may limit its use under certain geometrical and atmospheric conditions (low sun angles, shallow dive angles, low visibilities). The "cookbook" methods seem to offer obvious advantages. They are fast and do not require a large computer, high forecaster skill levels, or advanced knowledge of the radiative transfer process. But are they "good enough" to support AF operations? To answer this question, one must determine how good is "good enough." This, in turn, is dependent on how well AWS can forecast the variables that go into these simpler models. Clearly, a technique which depends greatly on a visibility forecast, for example, is of limited use if the visibility forecasting skill level is nil.

The techniques developed by Huschke (1976) hold the possibility of answering USAFETAC's search for an "appropriate forecast method" to support TV-guided PGMs. His method has the advantage of employing common meteorological observations plus estimates of target backgrounds and can be employed by either an individual remote forecaster or a centralized computer facility. This report attempts to verify the validity and comment on the possible future operational utility of the Huschke model by comparing its output with that of three theoretical computer models under similar meteorological and geometrical conditions. The intercomparison of the three theoretical models is, of course, involved. Since most of the 5th Weather Wing techniques duplicate the Huschke method, the results of this study will also apply to them. Neither the "rapid" nor the more extensive methods described in the AWS EO Handbook (Cottrell, et.al., 1979) will be discussed here.

While the Huschke model and the theoretical computer models share some basic elementary assumptions and equations, each model treats the vertical structure of the atmosphere and other input variables in a different manner. These differences complicate the comparison process. The comparing "apples and oranges" aspects of this study have been reduced as much as possible, but some differences are endemic. A discussion of these differences follows.

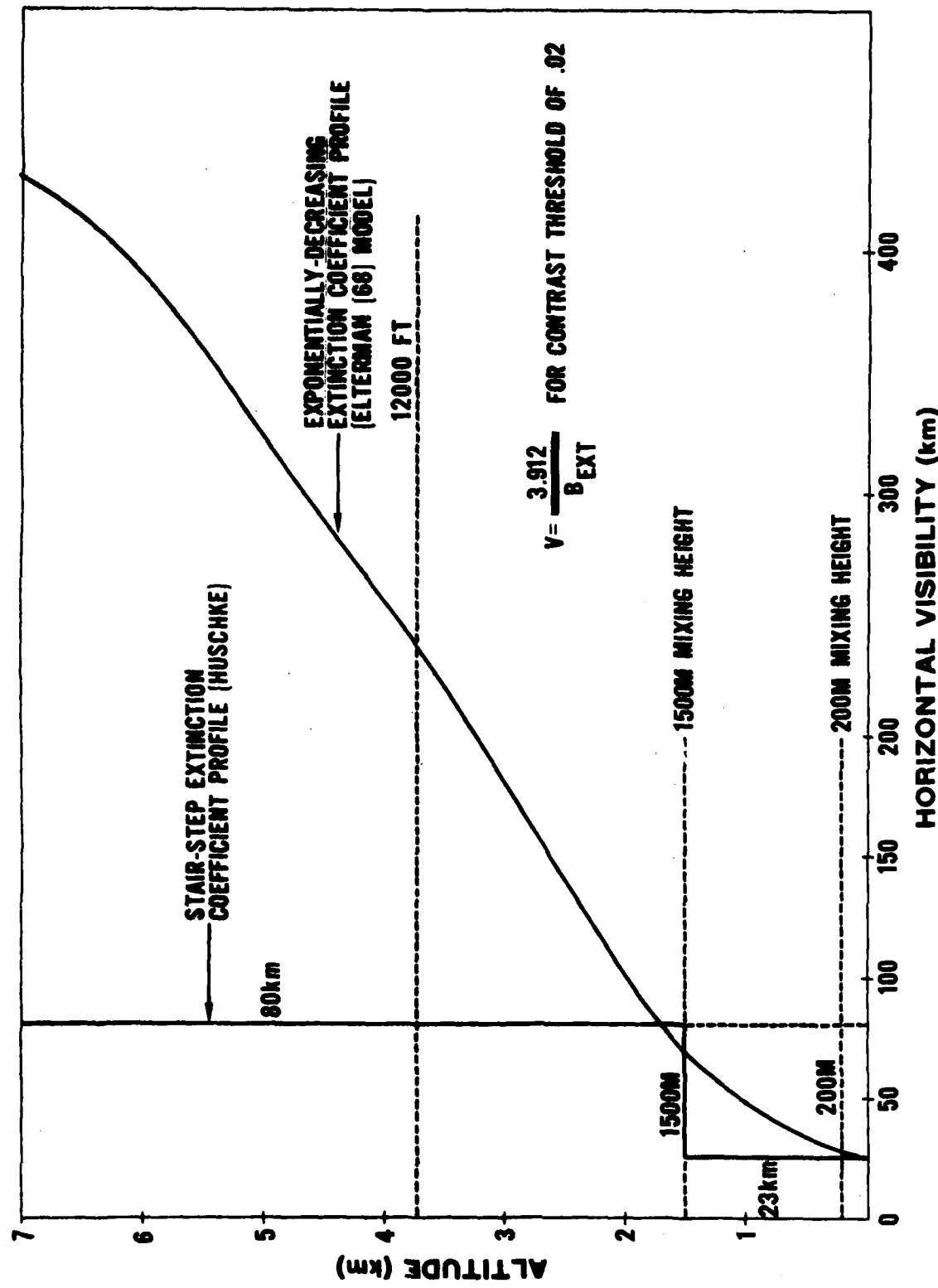


Figure 1. Horizontal Visibility Profiles for Stair-Step and Exponential Extinction Coefficient (23-km surface visibility).

The principal feature of the Huschke model (and one easy to misinterpret) is the determination of the vertical structure of the atmosphere from the decision tree (Huschke, 1976, page 21). Basically, Huschke views the atmosphere as being composed of two layers: a lower layer with the surface visibility extending to the top of the mixing layer, and an upper layer extending to the top of the atmosphere with a visibility of 80 km. The top of the mixing layer is either 1500 meters, 200 meters for clear sky, low wind, and low sun conditions, or at the base height of any clouds between 200 meters and 2500 meters. Since radiative transfer models such as FLASH, DART, etc., cannot treat partly cloudy conditions, this study must be limited to clear skies only. For a TV sensor above the mixing layer, the contrast transmittance, T_c , must be computed for the slant path of interest for each layer, and their product is then the T_c for the entire path length. This Huschke "stair-step" treatment of the vertical structure of the atmosphere is different from all previous runs of the FLASH, DART, or AWS models, which assume an exponentially decreasing extinction coefficient from a surface value based on the surface visibility. Both a lack of funds and the nonavailability of a CDC 6600 computer precluded USAFETAC's modification of the FLASH software to treat a stair-step extinction coefficient profile. Output from the DART model for specified inputs were available, but the lack of a running, debugged version of the program prevented USAFETAC from modifying the program to include stair-step profiles. Since the AWS model was easily modified and fast running, both stair-step and exponential profiles were used to compute slant path contrast transmittance values for a TV sensor at 12,000 feet AGL. Figure 1 graphically depicts the difference between a stair-step (200-meter or 1500-meter mixing depth) profile versus an exponentially decreasing one for a surface visibility of 23 km. Note that for a mixing depth of 1500 meters the visibilities for the stair-step profile are smaller (extinction coefficients larger) than the exponential profile at all altitudes. Thus, one would expect (a priori) computed T_c values to be smaller using the stair-step, 1500-meter mixing depth profile. This subject will be discussed further in the following chapters.

Another bothersome factor in trying to compare the Huschke model with the three radiative transfer models is how each treats the visible spectrum. While the Huschke model computes contrast transmittance values that purportedly represent the photopic region of the visible spectrum, the other models compute T_c for individual wavelength intervals in the visible spectrum (0.40 to 0.75 microns). One could compute T_c values for several wavelength intervals and then numerically integrate them to give a T_c value for the visible. However, this would involve unacceptable computer run times for both the FLASH and DART models. A far more acceptable solution to this problem is to compute T_c values at 0.55 microns and then assume that such values approximate to an acceptable degree those for the entire photopic region. This assumption was tested using the AWS model to minimize computer run times. The T_c values for eight wavelength intervals (0.40, 0.45, 0.50, 0.55, 0.60, 0.65, 0.70, and 0.75 microns) were computed for a variety of geometrical inputs and background reflectances. These values were then numerically integrated (via a combination of Simpson's and Newton's 3/8th rules) and compared with the computed values at 0.55 microns. Figure 2 shows that, within the assumptions upon which the AWS model is based, computed T_c values for 0.55 microns do closely reproduce those for the entire visible wavelength region.

The azimuthal angle dependence of contrast transmittance is another factor which is treated differently by the Huschke model than the other types of models. The Huschke model computes a T_c which is not a function of the sun-target-sensor azimuthal angle while FLASH, DART, and AWS models compute a T_c which is a function of azimuthal angle. For certain sun and dive angles, this difference can be considerable. Figure 3 depicts the difference between T_c values for azimuthal angles of 0°, 90°, and 180° as computed from the FLASH model to demonstrate how large such differences can be. Note the large variation of T_c values with dive angle for a solar zenith angle of 60° and with dive angle for a solar zenith of 85°. To facilitate the comparison and evaluation of the models, computed values of T_c for 0°, 90°, and 180° solar azimuthal angles for FLASH, DART, and AWS were averaged $[(T_c(0^\circ) + T_c(90^\circ) + T_c(180^\circ))/3]$ and this mean value was then compared with the Huschke-derived values for the same geometry. While a weighted mean would probably have had more validity, no acceptable method of choosing such weights could be found.

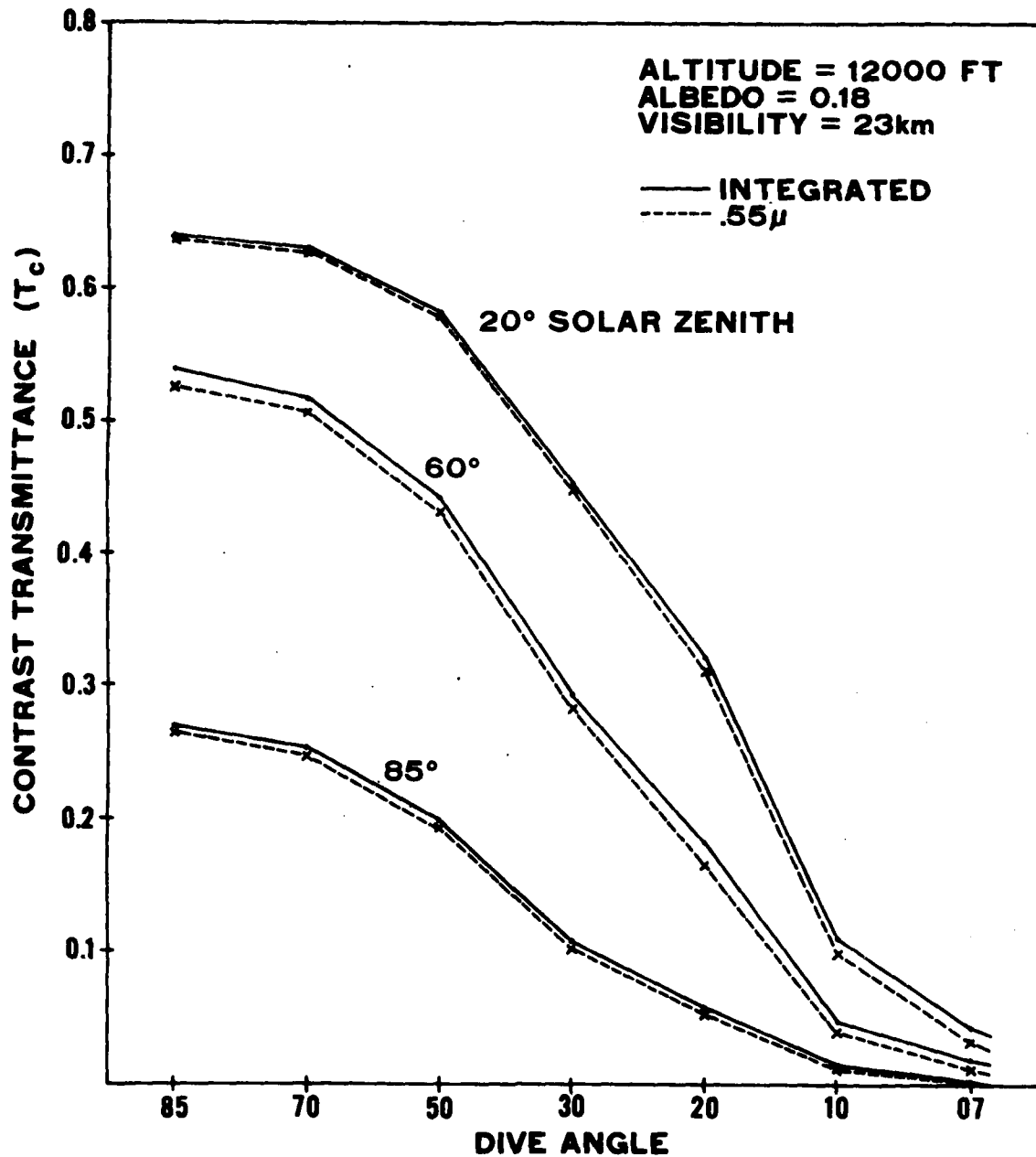


Figure 2. Comparison of Contrast Transmittance Integrated over Eight Wavelength Intervals with the Contrast Transmittance for 0.55 Microns.

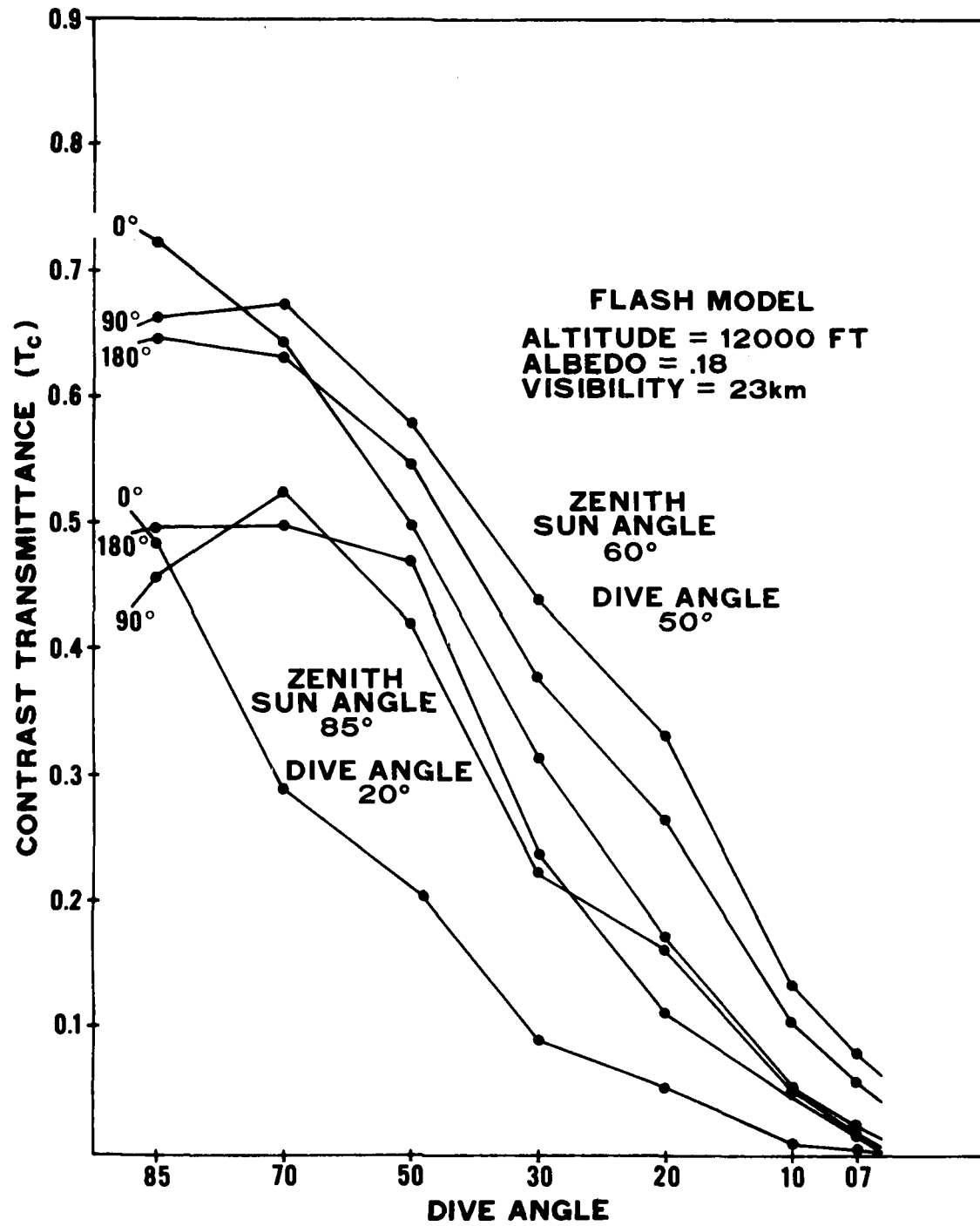


Figure 3. Variation of Contrast Transmittance with Azimuth Angle for FLASH Model.

In addition, Huschke computes visible extinction coefficients using the equation $\beta = 3.352/\text{Visibility}$, whereas the other models use the more common relationship $\beta = 3.912/\text{Visibility}$. This results in Huschke-inferred visible extinction coefficients being about 15 percent lower than the other models (see Huschke; 1976, pages 7 and 8).

The other important input variables, dive or depression angle, solar elevation or zenith angle, surface albedo, and visibility were the same for all models. However, Huschke (1976) treats specific values of these variables as belonging to a particular category as input to an algorithm to compute the sky-ground ratio, while the other models employ the values of these variables directly as input.

In summary, this study will compare the contrast transmittance values as computed from the FLASH, DART, and AWS models for clear sky conditions and

- a. One altitude, 12,000 feet AGL
- b. Two mixing depths, 200 meters and 1500 meters
- c. Two visibilities, 23 km and 5 km
- d. Three solar zenith angles, 20° , 60° , and 85°
- e. Three albedos, 0.06, 0.18, and 0.80
- f. Seven dive angles, 85° , 70° , 50° , 30° , 20° , 10° , and 7° (0° is level flight, 90° is straight down).

The vertical attenuation coefficient profiles at 0.55 microns for 23 km and 5 km were taken from Elterman (1970 and 1968).

Chapter 3
CONTRAST TRANSMITTANCE COMPARISON FOR 23 KM

The figures which follow in the remainder of this report employ a common notation. FL denotes the results of the Air Force Geophysics Laboratory's (AFGL) FLASH Monte Carlo model with an exponential extinction coefficient profile (Elterman 1968). DT stands for the Draper Lab's DART model with the same profile as input. H1 is output from the Huschke model with a mixing depth of 200 meters and a layered or stair-step extinction coefficient profile. H2 represents output from Huschke's model for a mixing depth of 1500 meters. A1 refers to the results of the AWS Haze Model with an exponential (Elterman, 1968) profile while A2 is for a stair-step extinction coefficient profile with a mixing depth of 1500 meters.

Figures 4, 5, and 6 depict the variation of computed contrast transmittance for the various models for an albedo of 0.18 and solar zenith angles of 20°, 60°, and 85°. An element common to all these figures is that the Huschke model values bracket nearly all the values for the other models with H1 showing the most optimistic T_c values and H2 showing the most pessimistic. This trend parallels the total optical depth below the sensor for the various models with H1 having the smallest and H2 the largest values of all the models. A discrepancy in the Huschke model is apparent in Figures 5 and 6. At nearly vertical dive angles (85°) the Huschke model predicts T_c values which are considerably less than for a 70° dive angle. This aspect of the Huschke model is not shared by any other model. It is due to the way that F_{δ} is found from Tables 3 and 4 of Huschke's (1976) report which in turn are based on measurements of the sky-ground ratio published by Duff (1972). The footnote below Table 4 restricts F_{δ} to a value of 1.0 for dive (depression) angles between 50° and 82°. However, for dive angles greater than 82°, F_{δ} is allowed to take on values larger than 1.0. This larger value of F_{δ} can result in a larger value of the sky-ground ratio estimate, SG, which then results in the calculation of a T_c value for 85° that is less than that for 70° for certain solar zenith angles. While Duff's measurements seem to support this anomaly, all other evidence points to the situation whereby the contrast transmittance is at a maximum for nadir dive angles and decreases in value as one looks toward smaller dive angles near the horizon. This is one aspect of the Huschke model that will require further investigation.

Figures 7a and 7b more clearly show the differences between various pairs of models. Plotted are the percentage differences

$$\frac{T_c^1 - T_c^2}{T_c^1} \times 100$$

between contrast transmittance values for each of several dive angles for a solar zenith angle of 20° and an albedo of 0.18. The Huschke model with a mixing depth of 200 meters (H1) agrees best with the AWS model (A1) and quite well with the FLASH and DART models, with a gradual fall off in agreement as one approaches near-horizon dive angles. The H1 shows T_c values that are consistently higher than FLASH as one would expect since its surface-to-sensor optical depth is smaller. On the other hand, there is no apparent reason why A1 with the same optical depth and aerosol model as FL should show consistently higher T_c values than FLASH. The Huschke model with a 1500-meter mixing depth (H2) compares less favorably with FLASH, especially at dive angles less than 30°. Once again, its greater optical depth accounts for some of the variation. Figure 7a shows that the percentage difference between H2 and FLASH and DART gradually increases with decreasing dive angle, becoming greater than 100 percent near the horizon. Figure 7b again shows the Huschke/AWS comparison (H1,A1) along-side the comparisons of the other models with one another. Most notable is the fact that, as the optical depth increases for smaller dive angles, the AWS model compares less and less favorably with FLASH and DART (although not as badly as Huschke). Percentage difference plots for solar zenith angles of 60° and 85° show similar trends.

Figures 8, 9, and 10 show the variation of T_c with dive angle for the various models for an albedo of 0.06 and solar zenith angles of 20°, 60°, and 85°. Figures

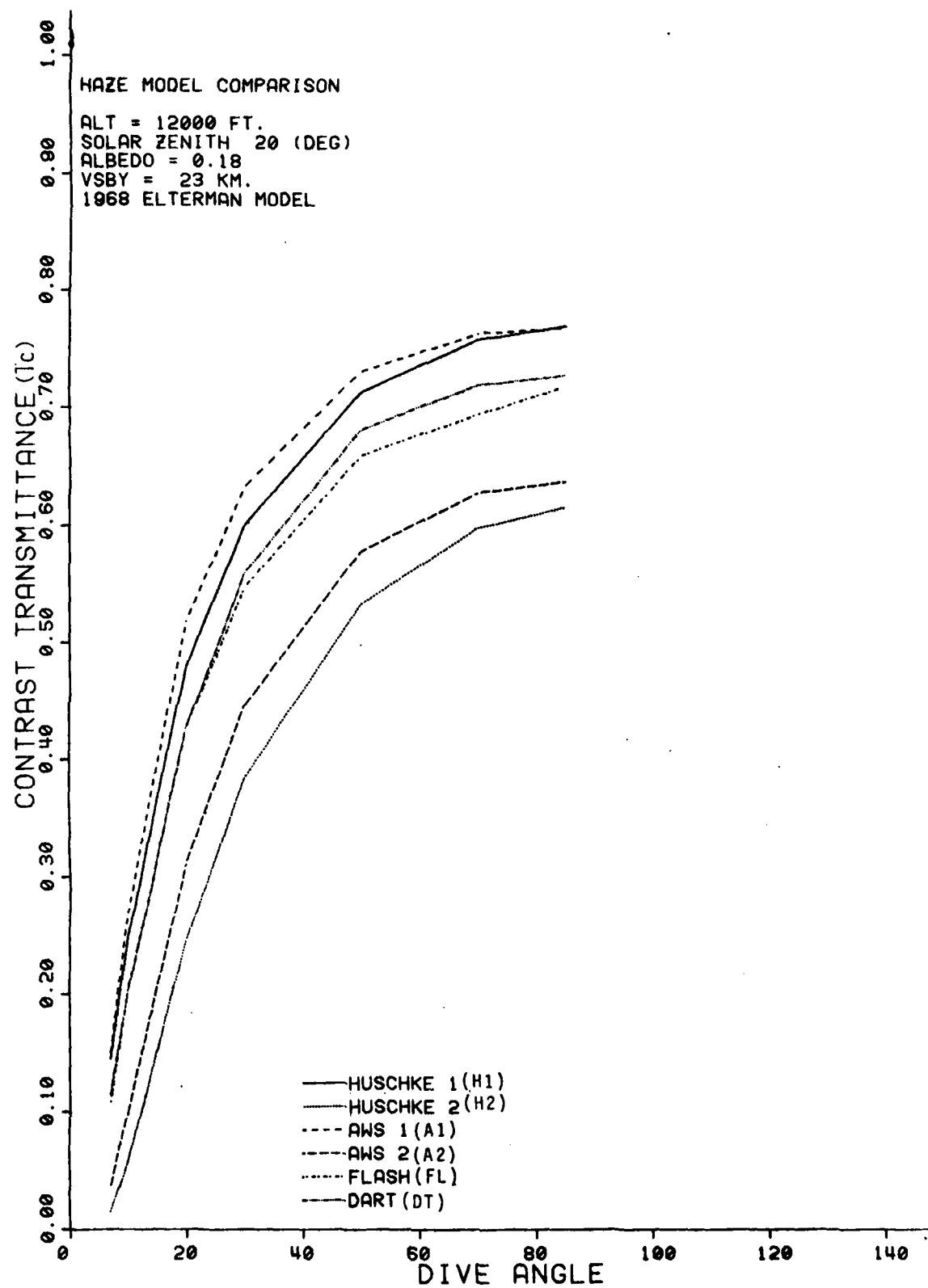


Figure 4. Contrast Transmittance at 20 Degrees Solar Zenith, Albedo of 0.18, and 23-km Surface Visibility.

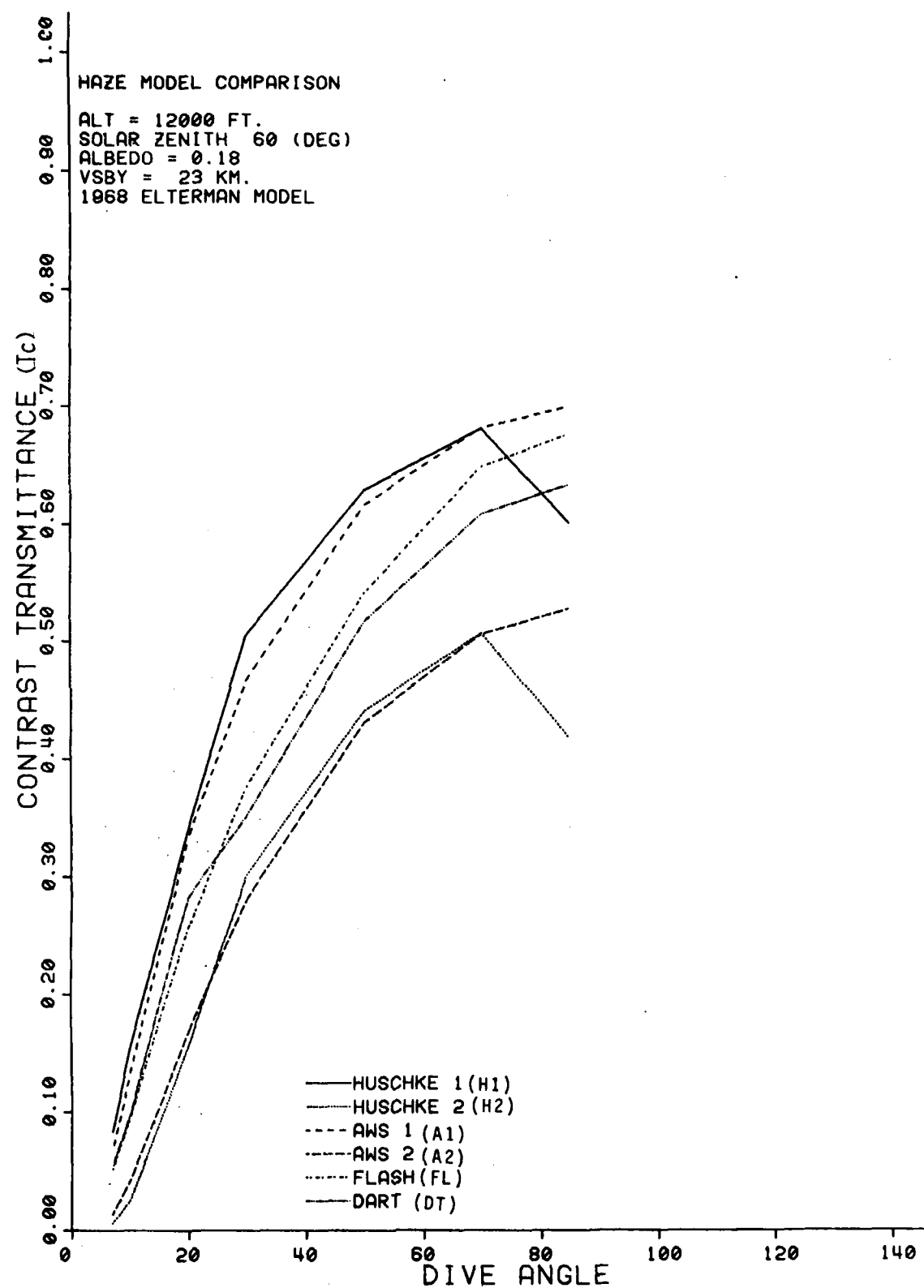


Figure 5. Contrast Transmittance at 60 Degrees Solar Zenith, Albedo of 0.18, and 23-km Surface Visibility.

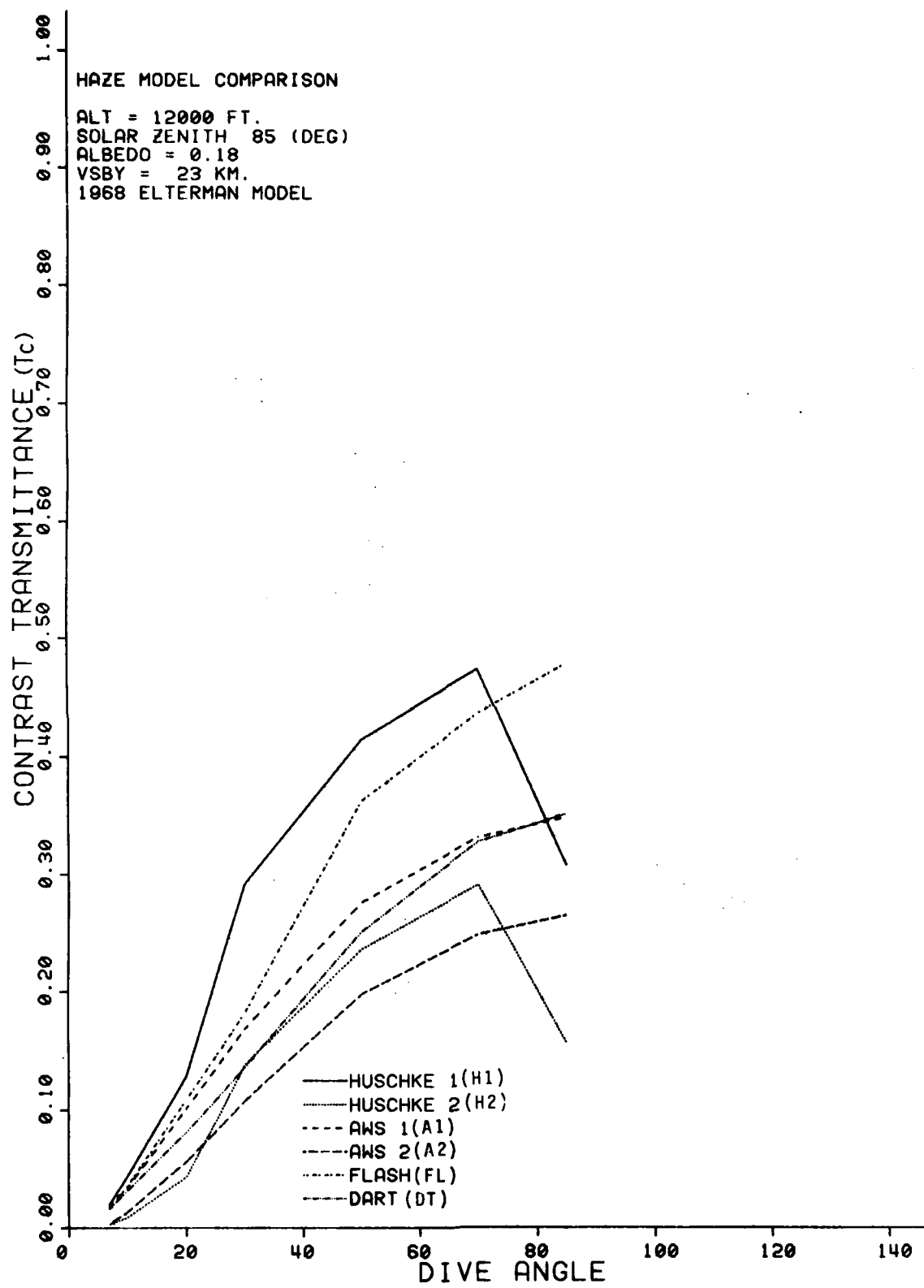


Figure 6. Contrast Transmittance at 85 Degrees Solar Zenith, Albedo of 0.18, and 23-km Surface Visibility.

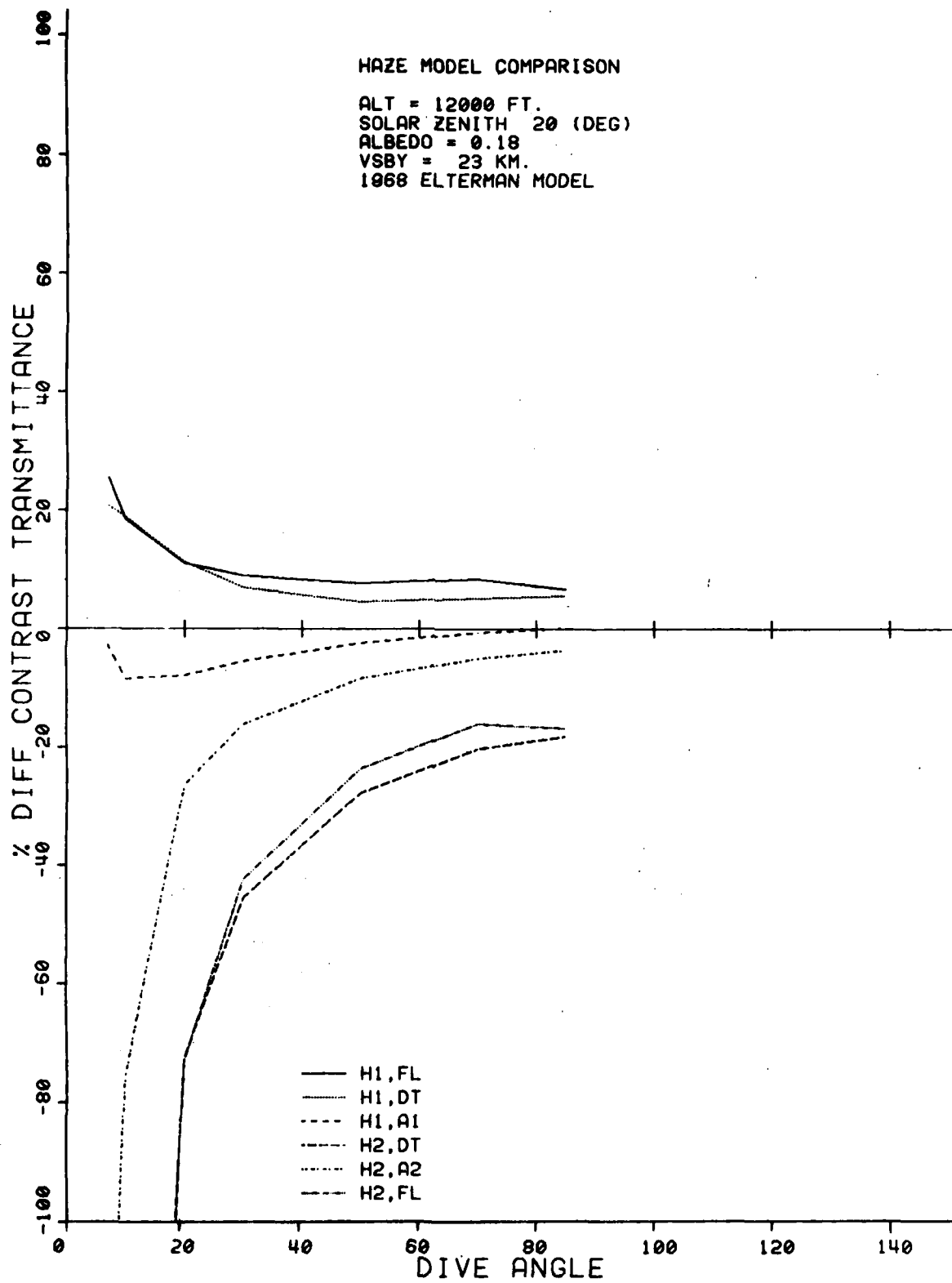


Figure 7a. Model Comparisons at 20 Degrees Solar Zenith, Albedo of 0.18, and 23-km Surface Visibility.

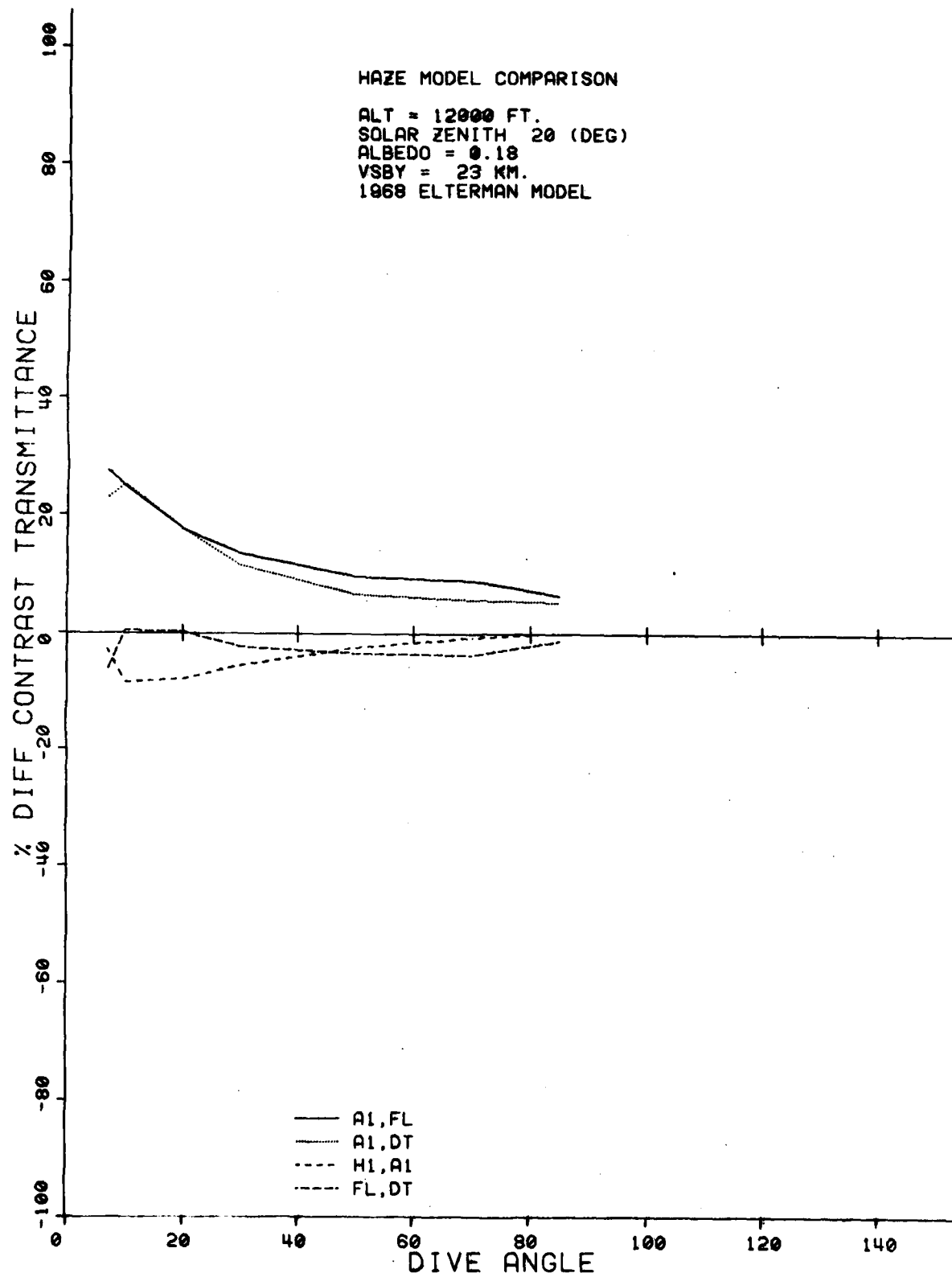


Figure 7b. Model Comparisons at 20 Degrees Solar Zenith, Albedo of 0.18, and 23-km Surface Visibility.

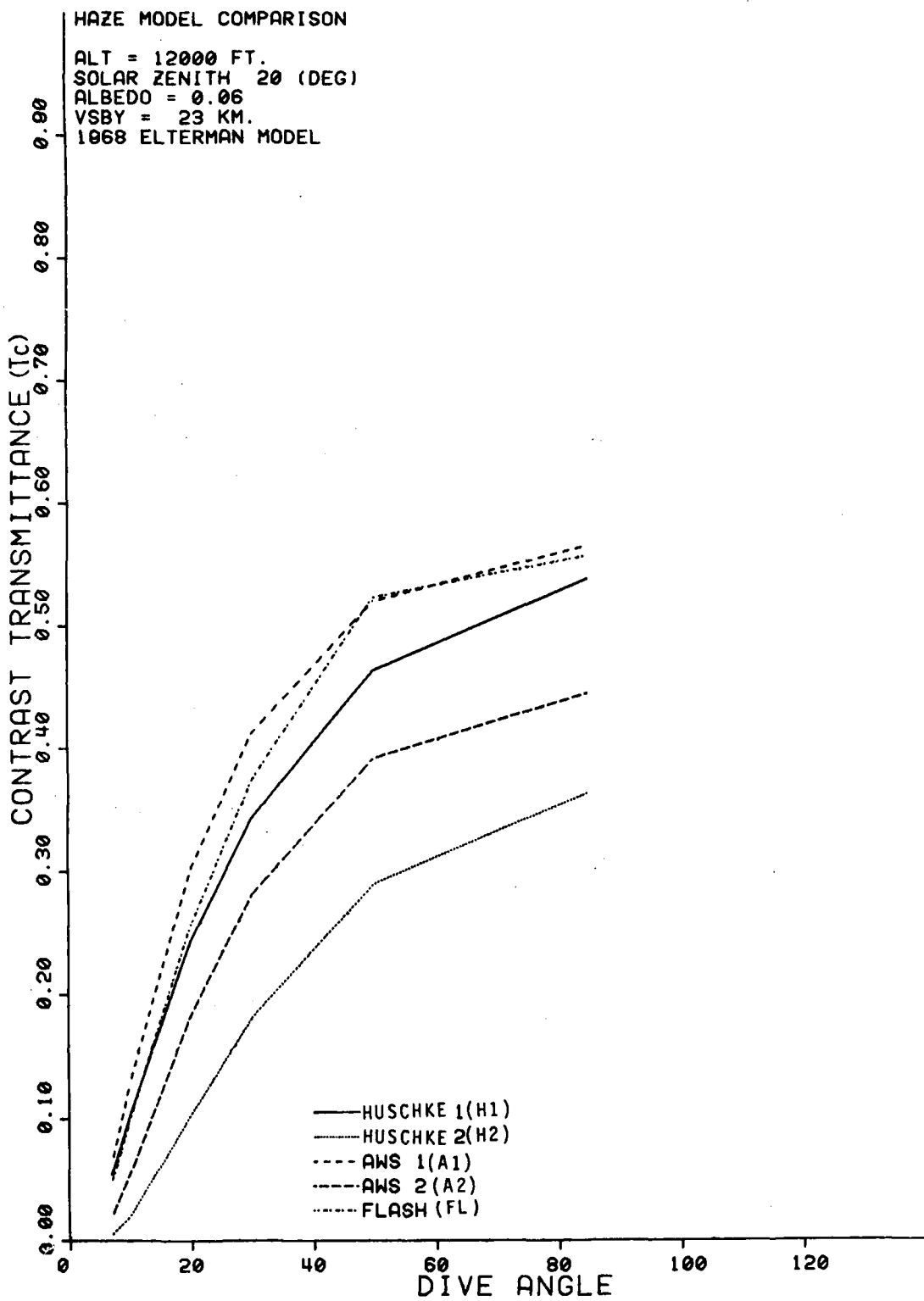


Figure 8. Contrast Transmittance at 20 Degrees Solar Zenith, Albedo of 0.06, and 23-km Surface Visibility.

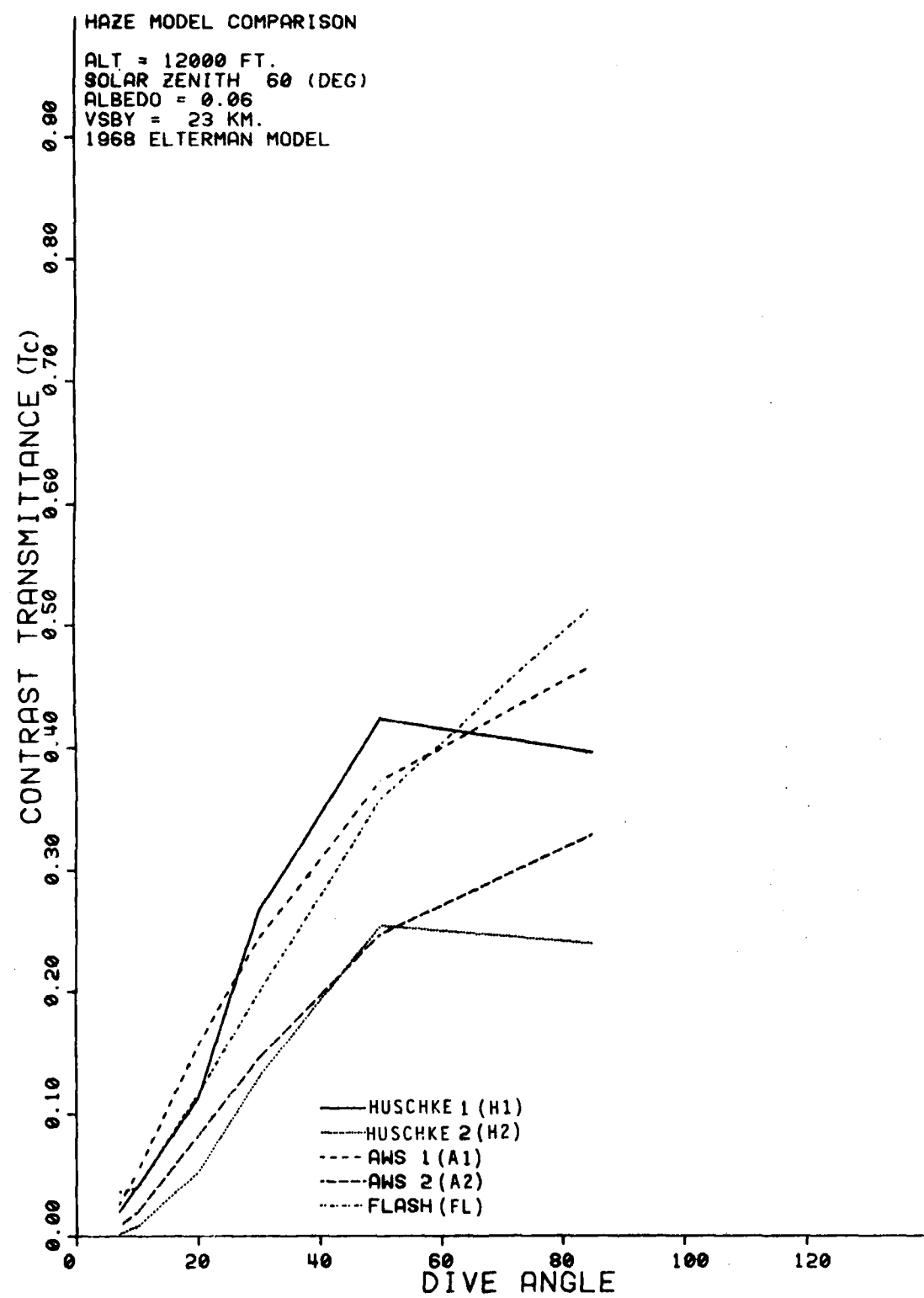


Figure 9. Contrast Transmittance at 60 Degrees Solar Zenith, Albedo of 0.06, and 23-km Surface Visibility.

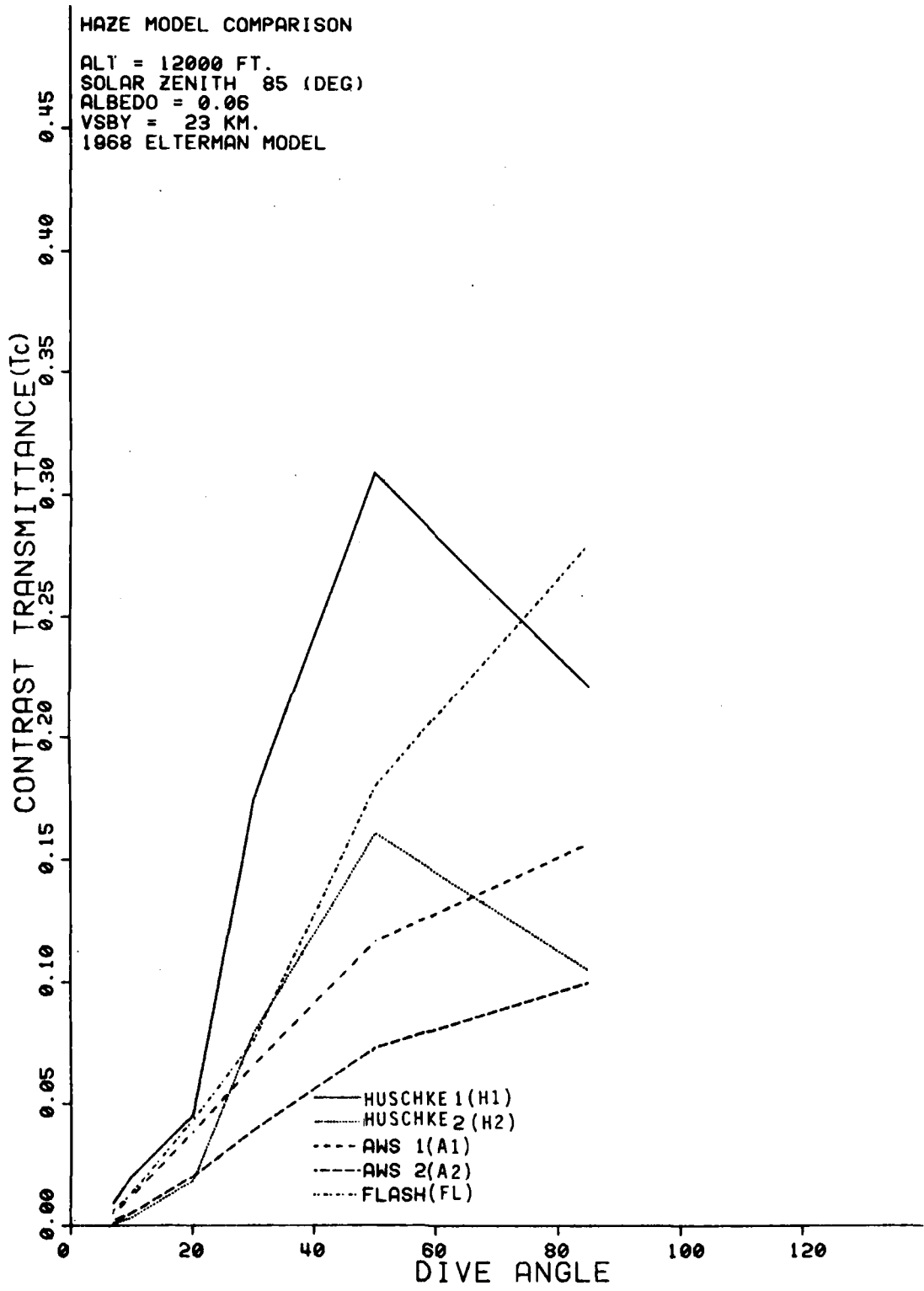


Figure 10. Contrast Transmittance at 85 Degrees Solar Zenith, Albedo of 0.06, and 23-km Surface Visibility.

9 and 10 again show the discrepancy of the Huschke model for near vertical dive angles. Figures 11, 12, and 13 repeat the process but for a background albedo of 0.80 (approximating snow cover). Note that for low sun conditions (85°, Figure 13) the Huschke model (H1) now underestimates T_c values while it tended to overestimate such values relative to the other models for higher sun angles (20° and 60°) previously. Figure 14a compares the percentage differences between the two Huschke outputs (H1 and H2) with the other models for a different solar angle (60°). Once again, the AWS (A1) model compares best with the Huschke 200-meter model (H1) and the H2,FL and H1,DT model comparisons show differences of less than 30 percent. Also, the Huschke 1500-meter model (H2) compares less favorably with FL and DT for dive angles less than 30° showing differences of over 100 percent for dive angles less than 20°. The fact that all differences are negative for all model comparisons for an 85° dive angle (Figure 14a) can again be attributed to the sky-ground ratio problem at near nadir dive angles mentioned earlier. Figure 14b shows that the AWS (A1) model compares well with the FL and DT models, predicting, for all dive angles, T_c values that are more optimistic than the other models. Figures 15a and 15b show similar trends, except for a solar zenith angle of 85°. Figure 15b shows that, for situations where the sun is near the horizon, the DART model does not agree particularly well with FLASH even though both are compatible spherical earth models. While the AWS (A1) model predicted larger values than FLASH for sun angles of 20° and 60°, it now predicts T_c values considerably smaller than FLASH. This may be due in part to the fact that the AWS Haze Model is a flat-earth radiative transfer model. However, it does a better job of duplicating FLASH T_c values at small dive angles than at large ones, which is difficult to explain from either a theoretical or geometrical point of view. Additional percentage difference plots for other angles and albedos will not be included because they would be repetitious and add little to this report.

Figure 16 depicts a method of comparing the various models for all dive angles simultaneously as the mean of the squared differences between T_c values. The model comparison with the smallest root-mean-square error (RMSE) value represents the best overall intercomparison. Note that as the solar zenith angle increases, the RMSE values are generally smaller because of the effect of smaller differences between smaller values of contrast transmittance. Lines connecting similar comparisons for different sun angles demonstrate the sun angle effect. For example, the A1,FL RMSE value decreases from 20° to 60° and then increases for an 85° solar angle, failing, however, to match the general downward trend in RMSE values mentioned above. The Huschke 200-meter/FLASH (H1,FL) RMSE values continue to increase as the solar zenith angle increases. While the FLASH/DART RMSE values are smallest overall for both 20° and 60°, the RMSE values increase threefold at 85°.

Since all dive angles were weighted equally in the RMSE values for Figure 16 and since most PGM operations take place at shallow dive angles, the RMSE values were recomputed with the T_c values for 85° and 70° dive angles omitted. Figure 17 shows these new RMSE values as compared to the values when all seven dive angles were included. Note that while most model comparisons show larger RMSE values when the two largest dive angles were omitted (solar angle 20°), three comparisons (H2,A2; H1,A1; and FL,DT) show smaller values for a solar zenith angle of 60°. However, both the Huschke (H1) and AWS (A1) models evidence large increases in RMSE values when compared to FLASH at 60° leading one to expect that these two models share a common deficiency. This trend is reversed at an 85° sun angle as both Huschke and AWS evidence reduced RMSE values when the T_c difference values for 85° and 70° dive angles are not included. Such evidence might suggest that both these models may be biased toward both near-horizon sun and dive angles.

In summary, both the Huschke and AWS models do an adequate job of approximating FLASH contrast transmittance values for a surface visibility of 23 km. The inherent limitations imposed by comparing models with different vertical extinction profiles (and therefore optical depths) probably account for some of the comparison discrepancies. Figure 18 compares the total optical depth values (0.55 microns) below the aircraft altitude (12,000 feet) for an exponentially decreasing extinction coefficient profile (FLASH, DART, AWS) with the Huschke model for mixing depths of 200 meters and 1500 meters. The total optical depth for the Huschke 200-meter model (0.203) is based on a visibility of 23 km for the lowest 200 meters and a visibility of 80 km from there to 3.66 km. The total depth for the Huschke 1500-meter model (0.361) is similarly based on a visibility of 23 km up to 1500 meters and 80 km above that. Note that as the mixing depth is increased, the optical depth increases until it equals the value for FLASH, DART, and AWS (0.230) just above 400 meters.

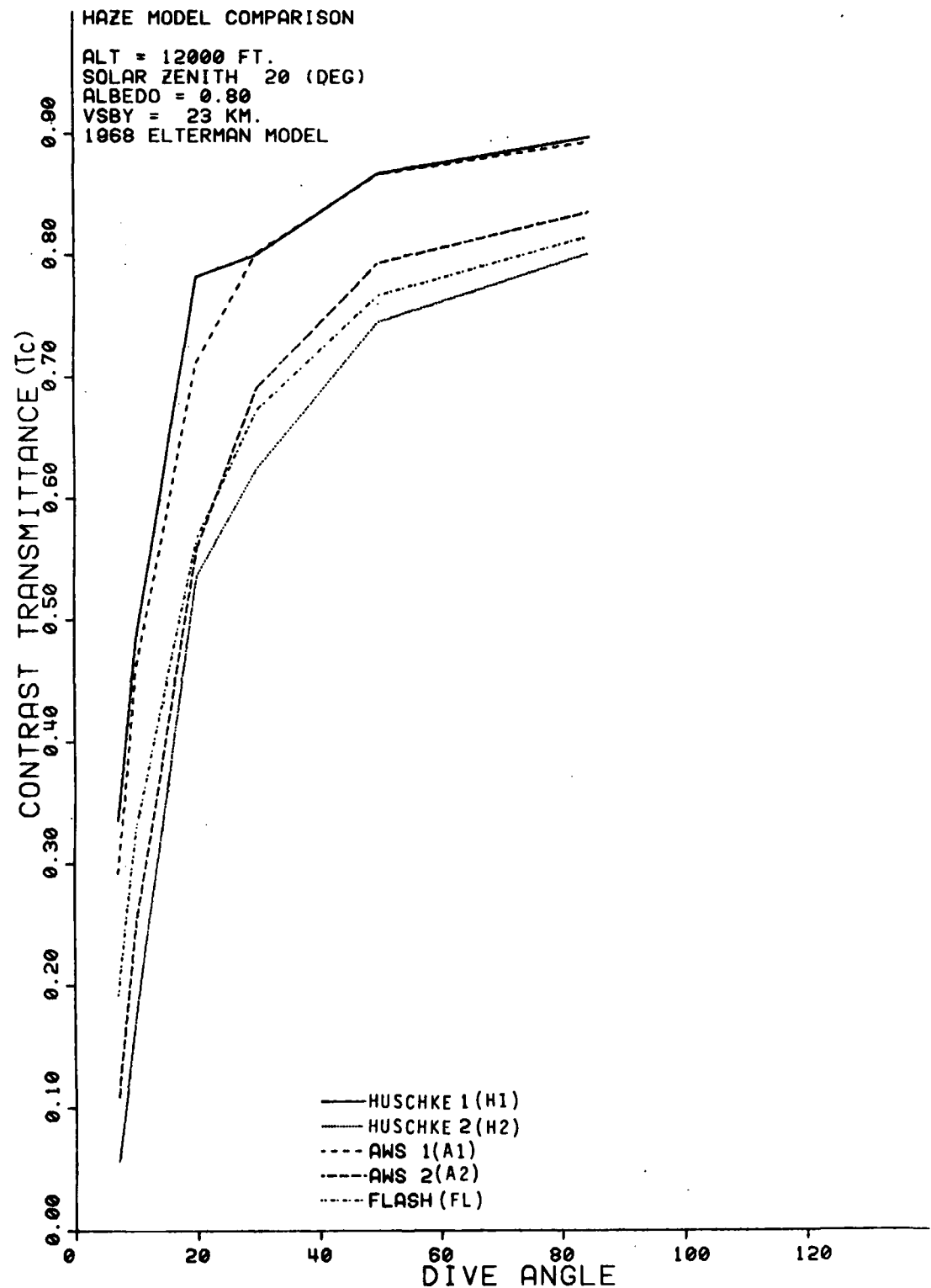


Figure 11. Contrast Transmittance at 20 Degrees Solar Zenith, Albedo of 0.80, and 23-km Surface Visibility.

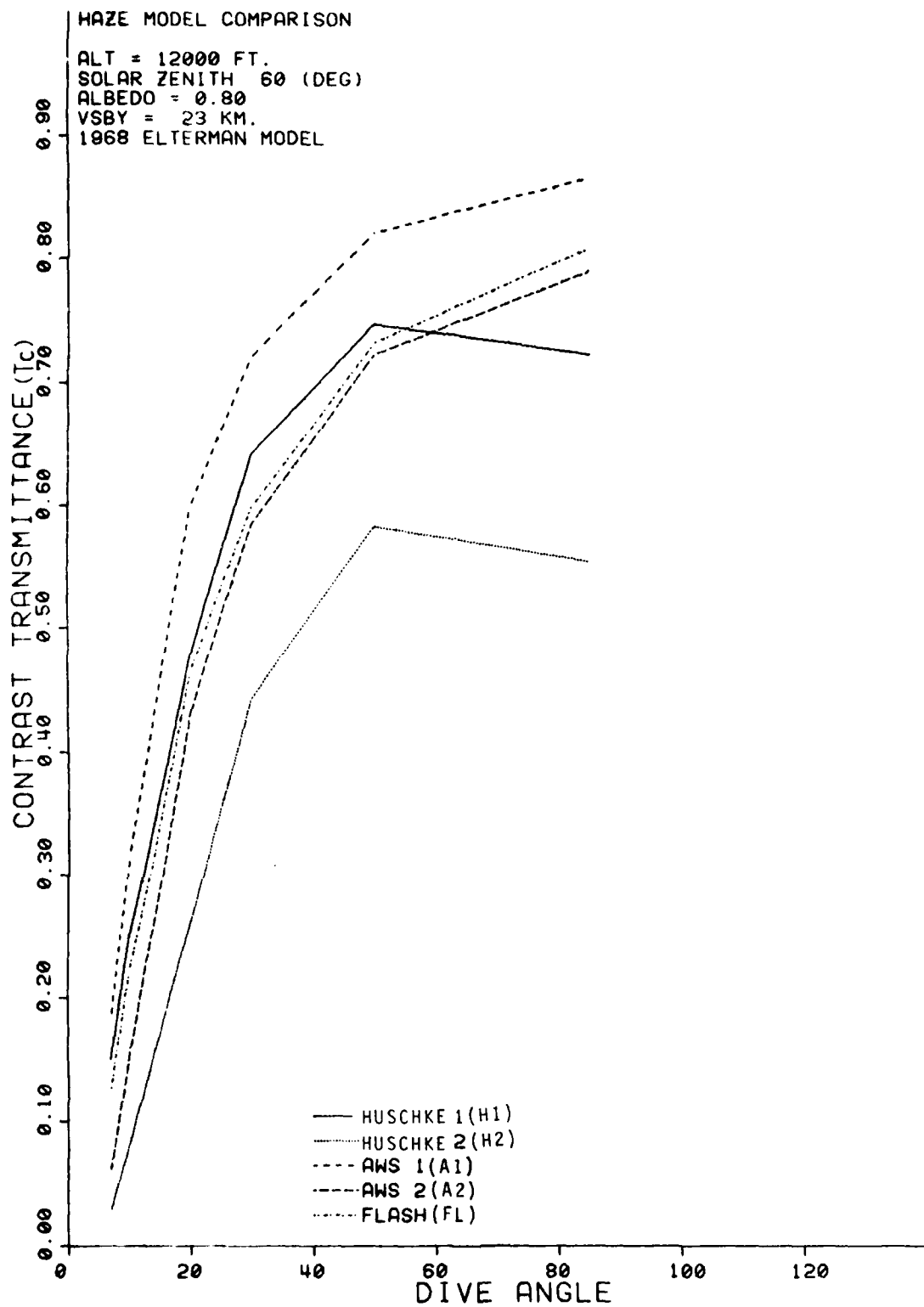


Figure 12. Contrast Transmittance at 60 Degrees Solar Zenith, Albedo of 0.80, and 23-km Surface Visibility.

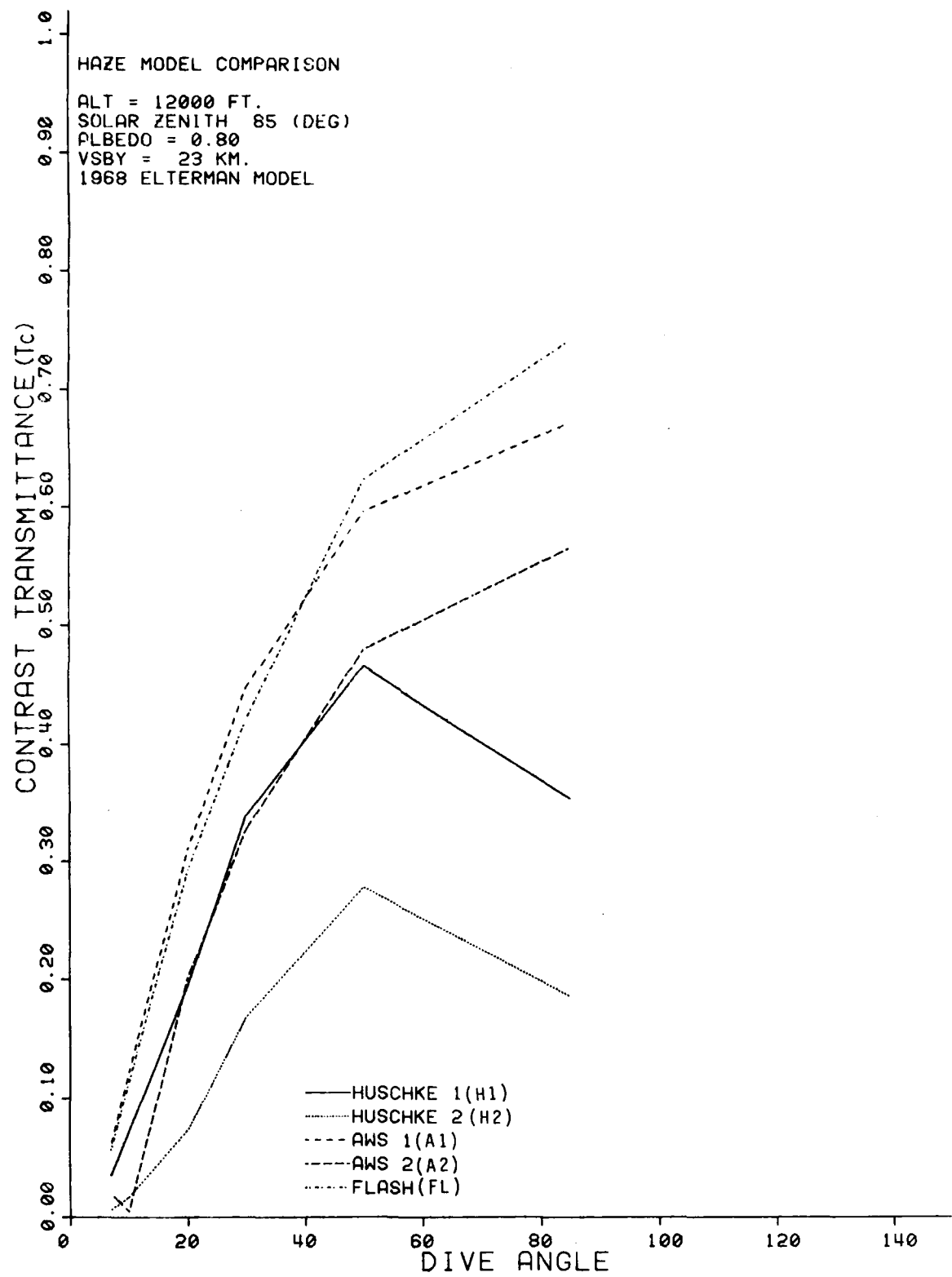


Figure 13. Contrast Transmittance at 85 Degrees Solar Zenith, Albedo of 0.80, and 23-km Surface Visibility.

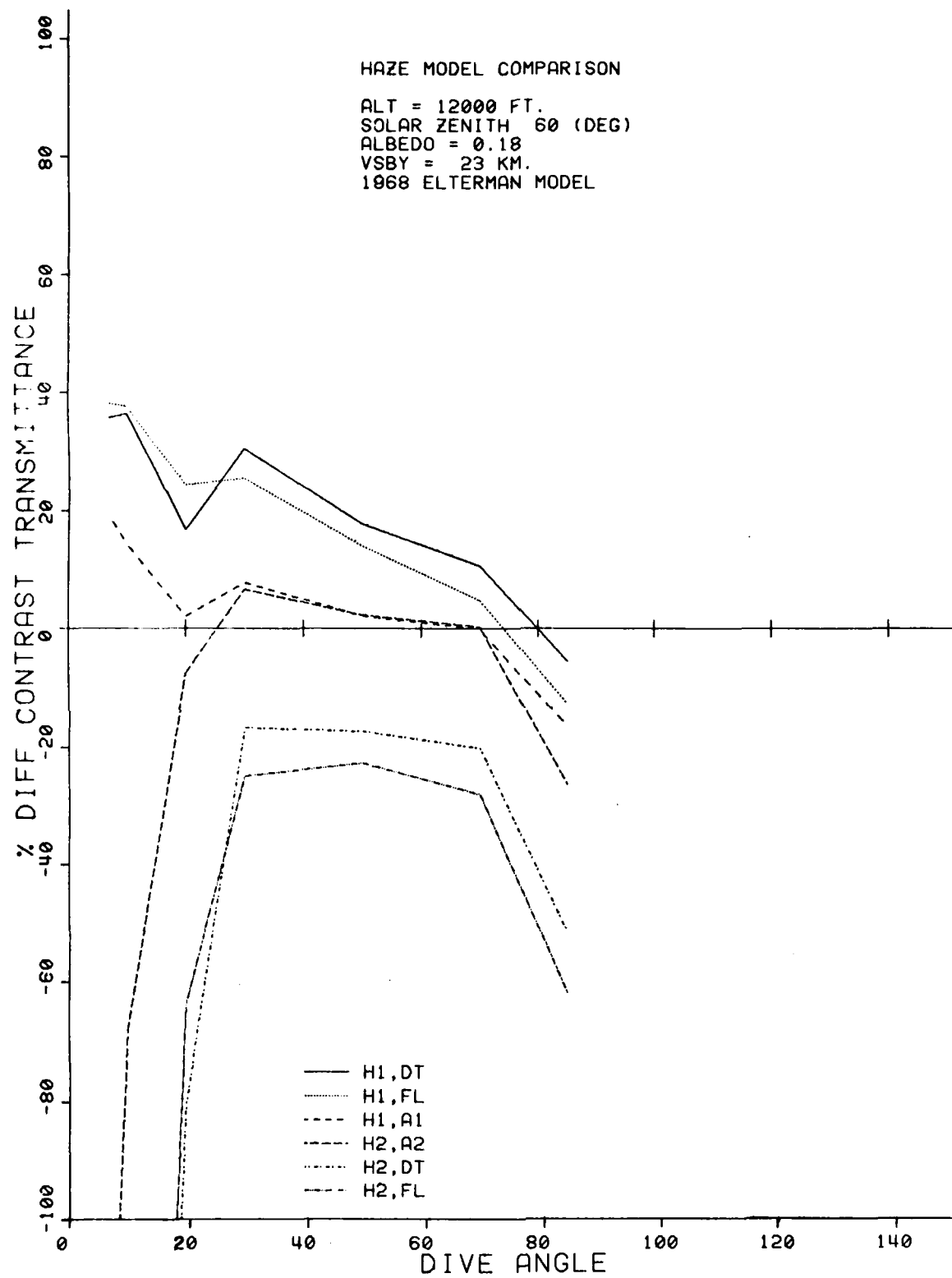


Figure 14a. Model Comparison at 60 Degrees Solar Zenith, Albedo of 0.18, and 23-km Surface Visibility.

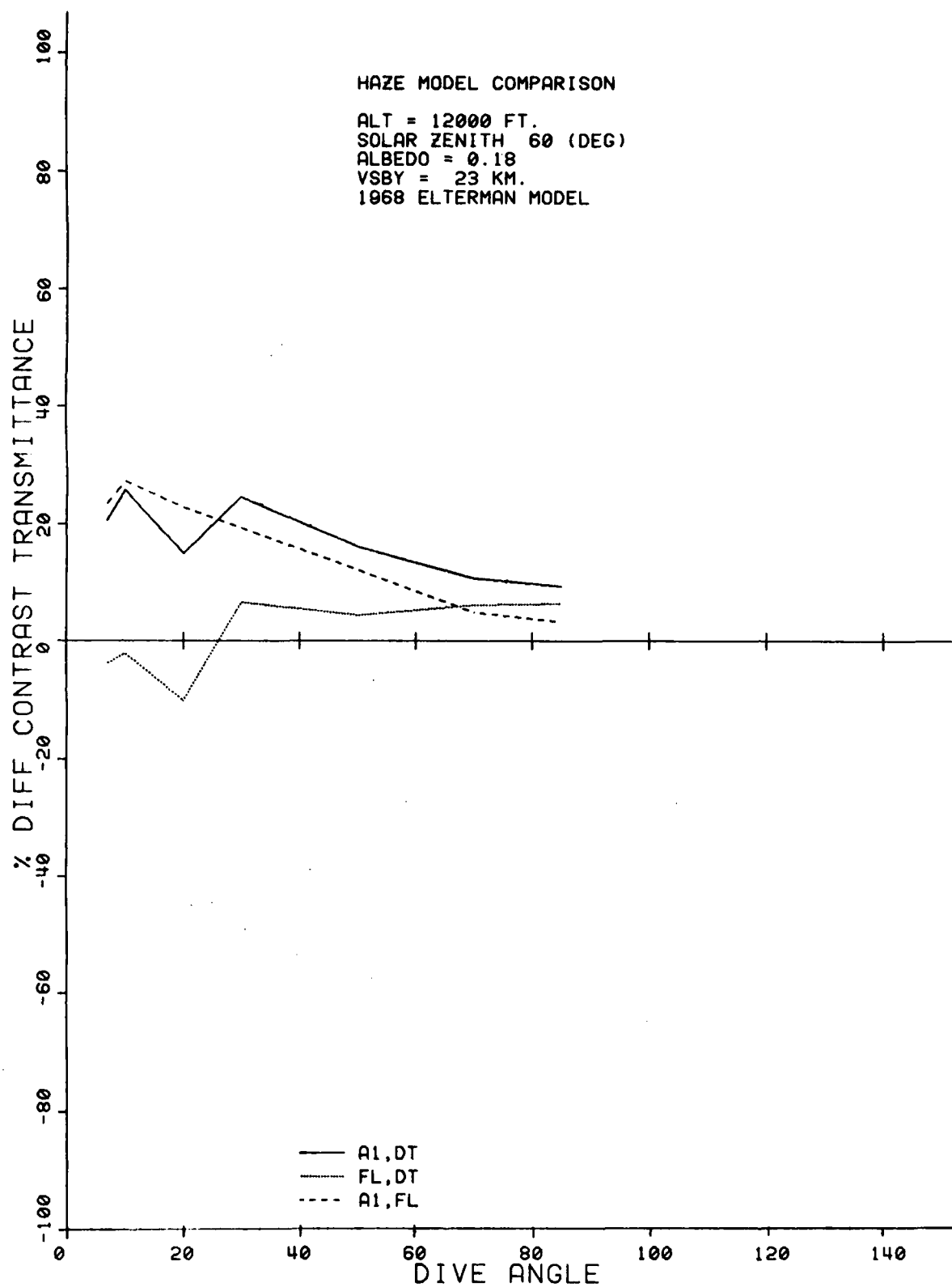


Figure 14b. Model Comparison at 60 Degrees Solar Zenith, Albedo of 0.18, and 23-km Surface Visibility.

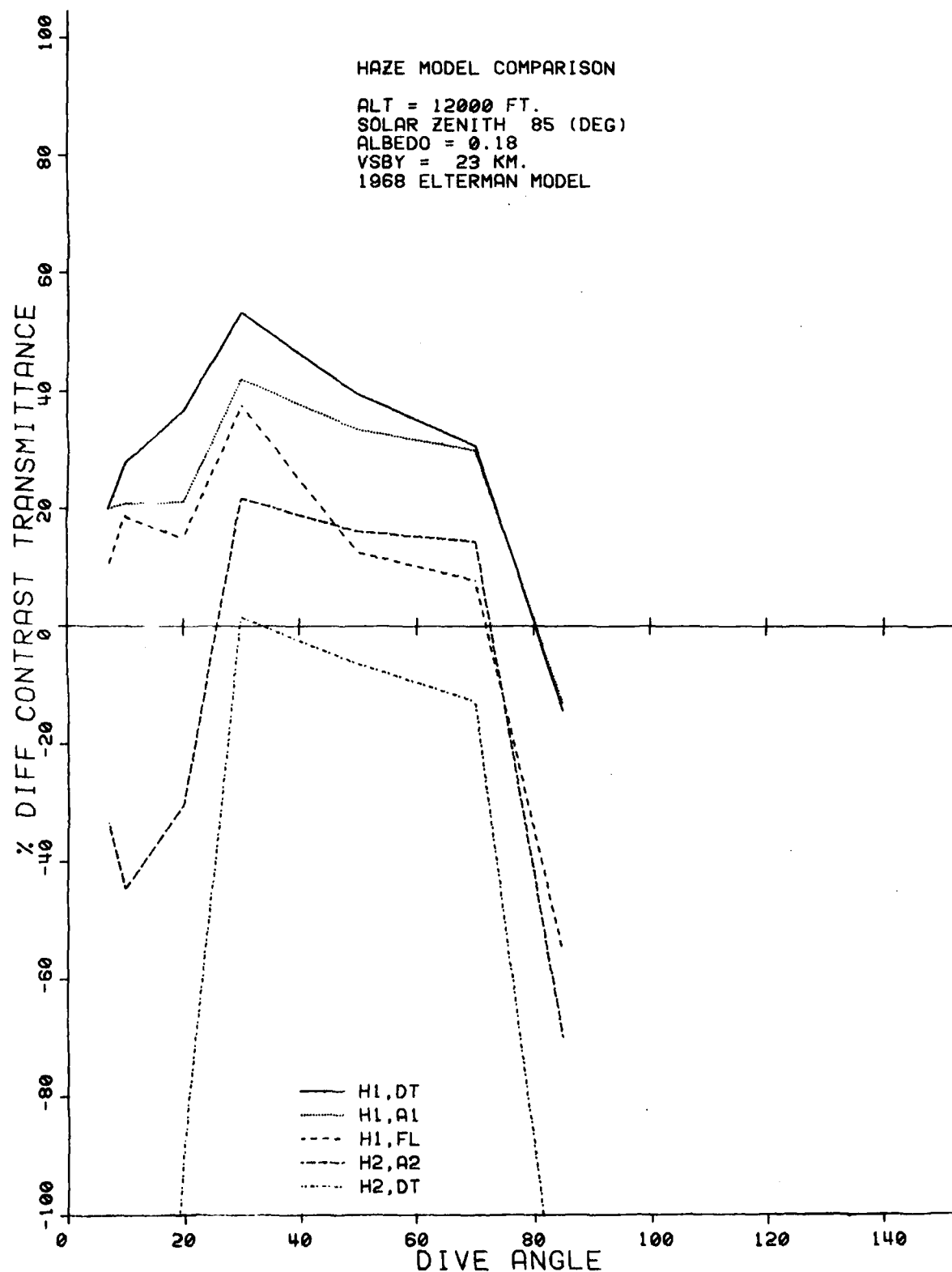


Figure 15a. Model Comparisons at 85 Degrees Solar Zenith, Albedo of 0.18, and 23-km Surface Visibility.

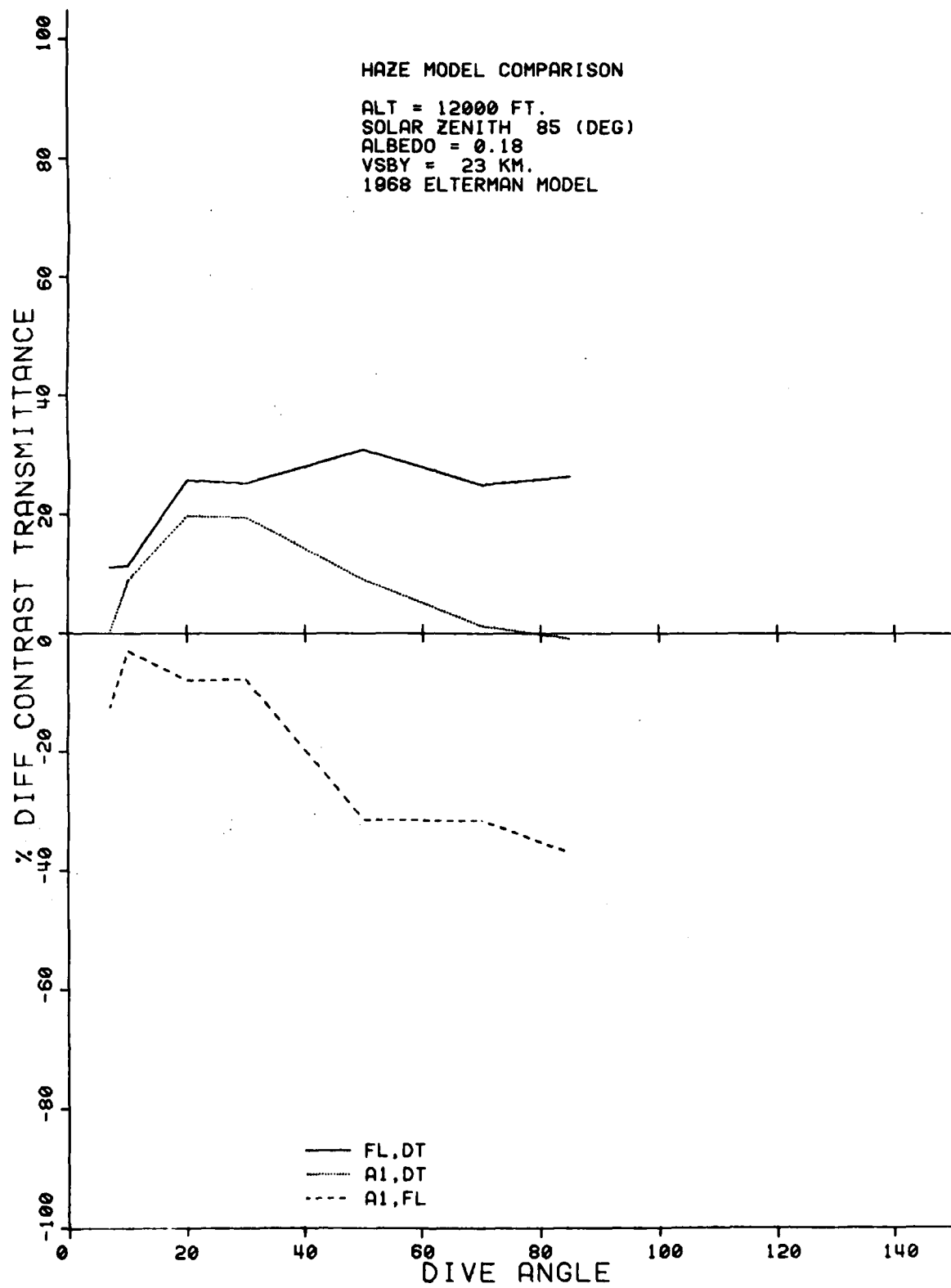


Figure 15b. Model Comparisons at 85 Degrees Solar Zenith, Albedo of 0.18, and 23-km Surface Visibility.

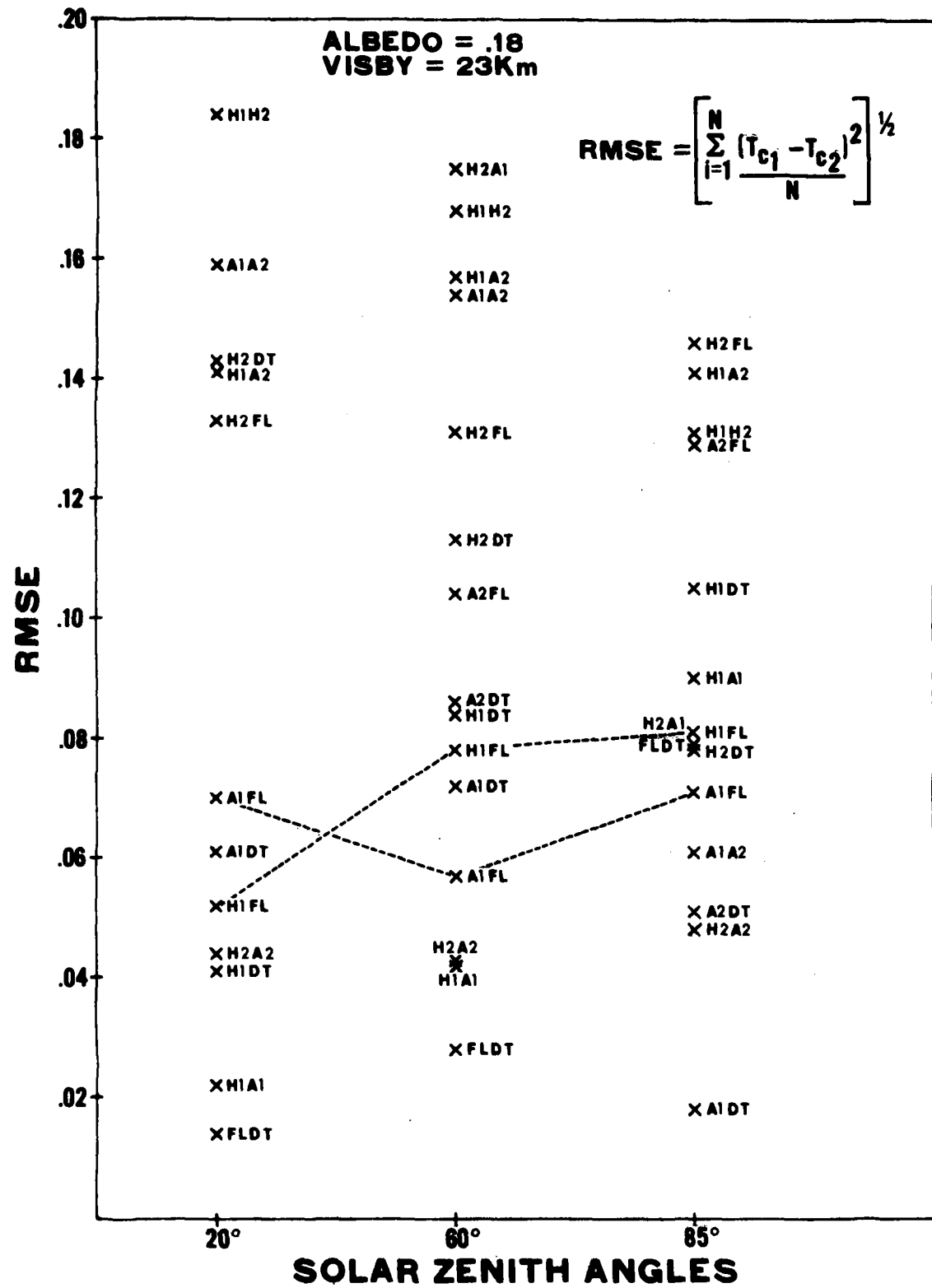


Figure 16. RMSE Model Comparisons for Albedo of 0.18 and 23-km Surface Visibility.

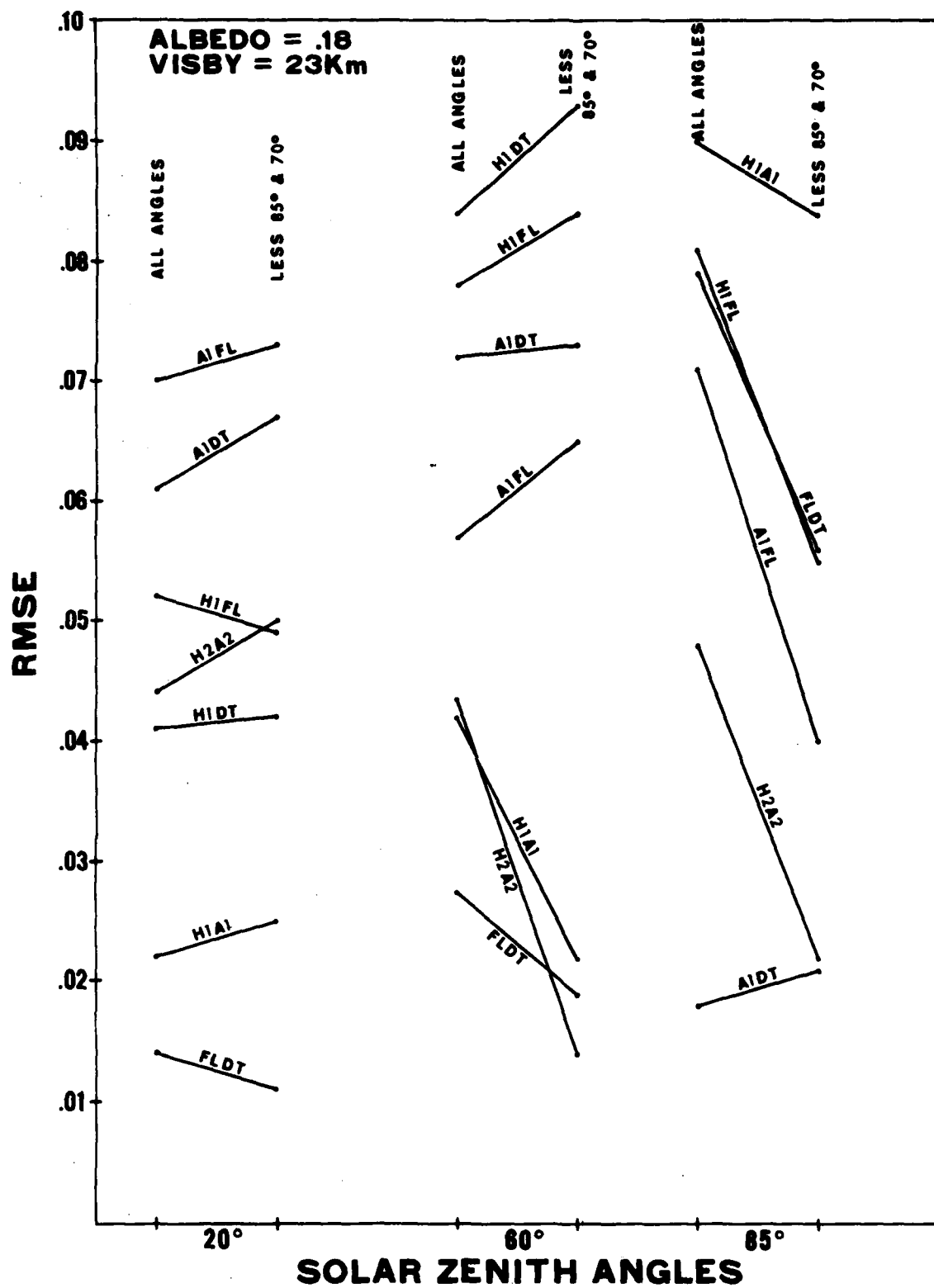


Figure 17. RMSE for All Solar Zenith Angles Versus RMSE without 85- and 70-Degree Solar Zenith Angles.

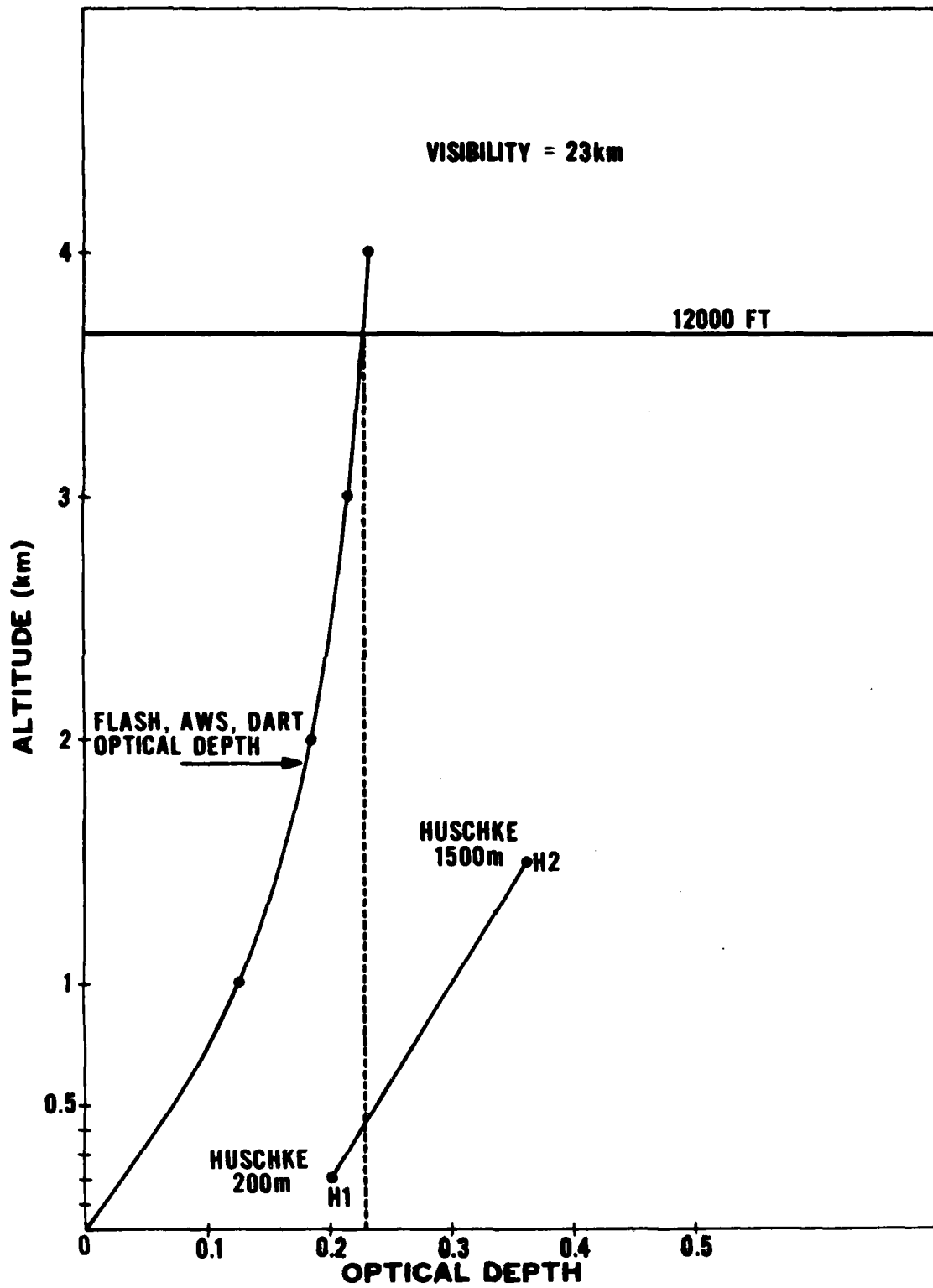


Figure 18. Total Optical Depth Below 12,000-Ft Viewing Altitude for 23-km Surface Visibility.

Thus, one would expect T_c values for H1 to be more optimistic than the other three models because of the smaller optical depth involved, and that H2 would produce more pessimistic T_c values because of the larger optical depth (0.361 versus 0.230). The tendency of some AWS model output to be more optimistic than FLASH at high sun angles and pessimistic at near-horizon sun angles is a cause for some concern. Also, the manner in which the Huschke model treats the sky-ground ratio for dive angles between 82° and 90° should be reexamined. Considering the fact that the Huschke and AWS models are hundreds of times faster than FLASH certainly argues in favor of further testing of these models at other surface visibilities. Such a comparison for a surface visibility of 5 km follows in the next chapter.

Chapter 4

CONTRAST TRANSMITTANCE COMPARISON FOR A 5-KM SURFACE VISIBILITY

While comparisons of radiative transfer models at larger surface visibilities (particularly 23 km) are fairly common, such a visibility is not representative of urban areas of the eastern US or central Europe. Much smaller surface visibilities usually prevail, particularly in the winter. A 5-km visibility was chosen as the other visibility for this study because it is much more representative of central Europe and probably also represents the lower limit of observed visibilities that will still allow successful TV-guided PGM operations.

The radiative transfer model designators used in Chapter 3 (H1, H2, A1, A2, FL, DT) apply again in this chapter with the exception of the DART model. No output data for this model for a visibility of 5 km are available at this time, or will be in the foreseeable future. Once again, the exponential extinction coefficients were taken from Elterman (1970). All other input variables were the same as before. Since computed contrast transmittance values for oblique dive angles at 5-km visibility tend to be very small, any T_c values less than 0.001 were considered as insignificant and were omitted.

Figures 19, 20, and 21 show the variation of contrast transmittance with dive angle for the five models for a solar zenith angle of 20° and background albedos of 0.06, 0.18, and 0.80, respectively. As they did for a visibility of 23 km, the two Huschke models bracket the T_c values for FLASH. The AWS exponential model (A1) evidenced considerably more variability with albedo than before. Once again, the total optical depth for FLASH lies between the values for H1 and H2. This point will be discussed more at the end of the chapter. A1 predicts slightly smaller T_c values than FLASH for an albedo of 0.06, much larger values for an albedo of 0.18, and then slightly larger values for an albedo of 0.80. Neither the 200-meter nor the 1500-meter mixing depth Huschke models approach the FLASH values for all three albedos. Figure 22 shows some of these differences more clearly. While the percentage differences between Huschke 200 meter (H1) and FLASH are fairly consistent (albeit large) throughout the range of background albedos, the AWS/FLASH (A1,FL) differences vary considerably with albedo, indicating a possible instability in the AWS model. The fact that A1 matches FL exactly at a 100° dive angle for albedos of 0.06 and 0.80 is not significant because of the small T_c value (0.002) involved.

Figures 23, 24, and 25 show the variation of contrast transmittance with dive angle and albedo for a solar zenith angle of 60° . Once again the two Huschke (H1 and H2) and AWS (A1 and A2) models bracket the FLASH model values with the AWS exponential model (A1) values showing the same variability with albedo as previously when the solar zenith angle was 20° . Only at a background albedo of 0.80 does the AWS exponential extinction coefficient model approximate the FLASH values. Figure 26 shows that none of the models does a good job of matching FLASH at all dive angles and albedos, with the Huschke 200-meter model (H1) showing a consistent bias toward optimistic T_c values. In general, the percentage differences between the Huschke and AWS models, vice FLASH, increase with decreasing dive angle, but the smallness of the T_c values for near-horizon dive angles make really meaningful comparisons suspect.

Figures 27, 28, and 29 repeat the comparison process for a solar zenith angle of 85° . The Huschke and AWS models again bracket FLASH for all three albedos with the Huschke (H1) values at near-nadir dive angles again different because of the way the model handles the sky-ground ratio estimate for these angles. As it did for a solar zenith angle of 60° , the AWS exponential model (A1) again is less than FLASH for an albedo of 0.06, greater than FLASH for an albedo of 0.18, and very nearly matches FLASH for an albedo of 0.80. Except for nearly nadir viewing, most T_c values for near-horizon sun angles are so small that it is doubtful that even high contrast targets could be acquired even at low aircraft altitudes. Figures 30 and 31 show that neither the Huschke nor AWS models do a good job of duplicating FLASH contrast transmittance values, although the AWS models show slightly more consistency and

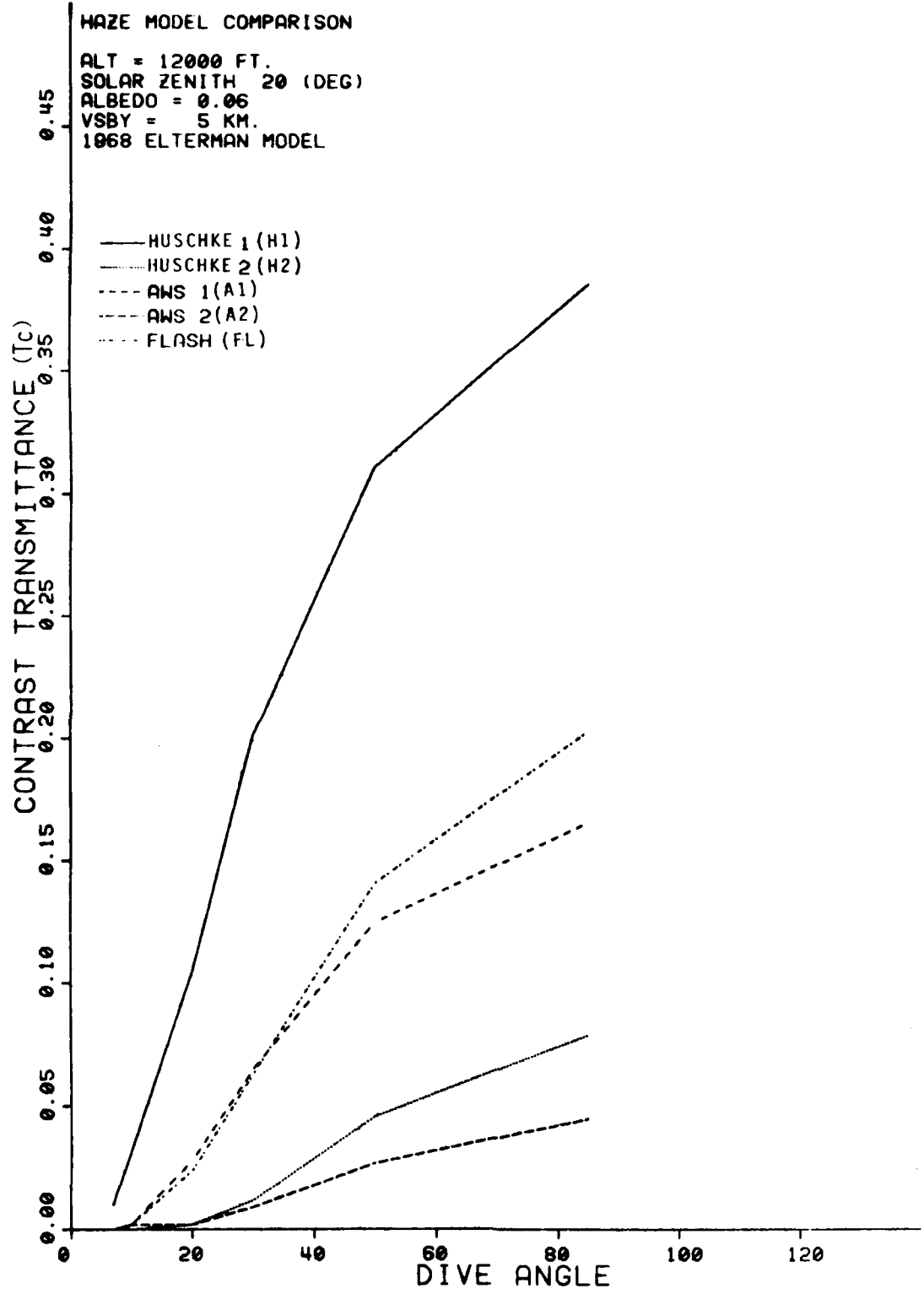


Figure 19. Contrast Transmittance at 20 Degrees Solar Zenith, Albedo of 0.06, and 5-km Surface Visibility.

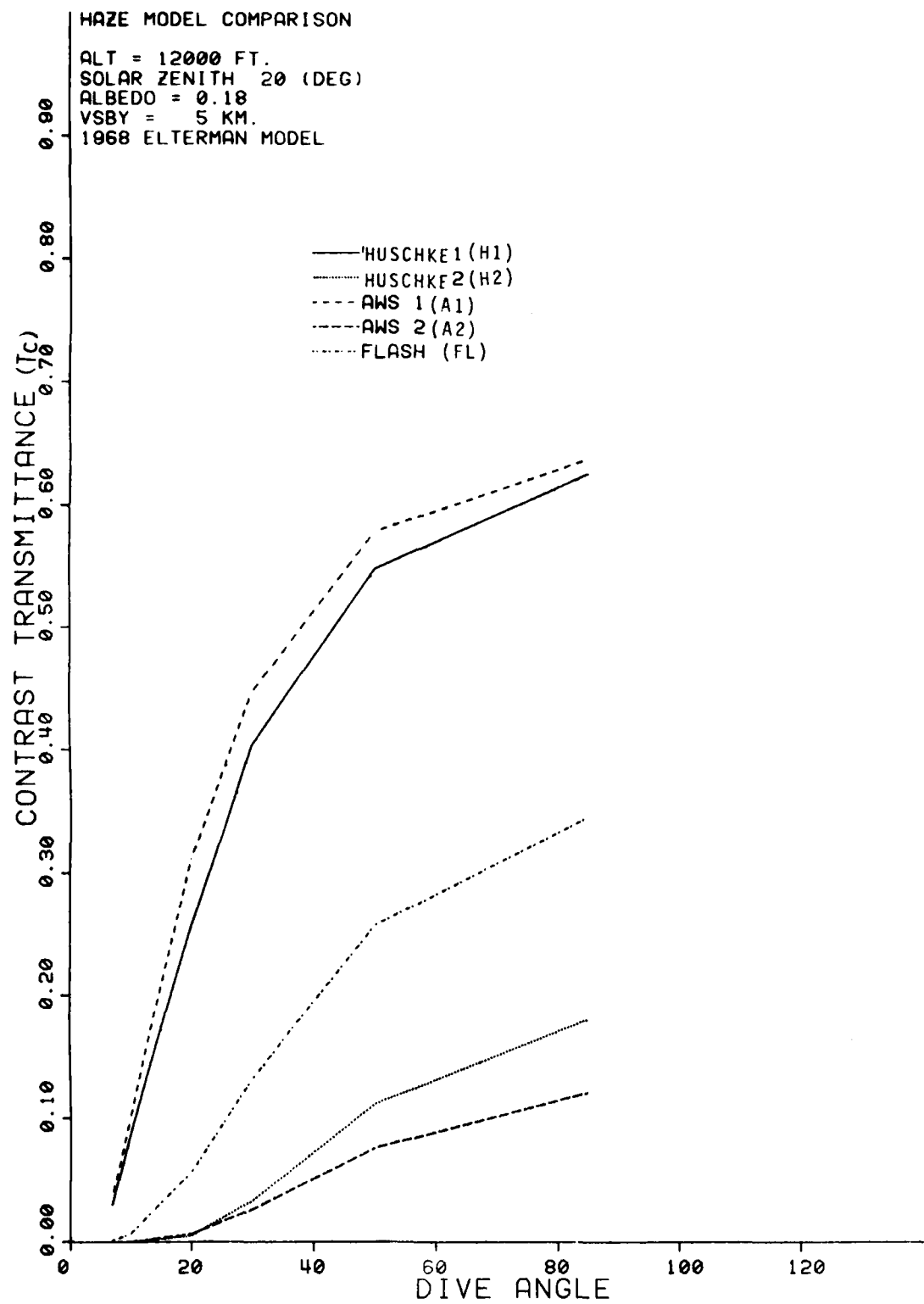


Figure 20. Contrast Transmittance at 20 Degrees Solar Zenith, Albedo of 0.18, and 5-km Surface Visibility.

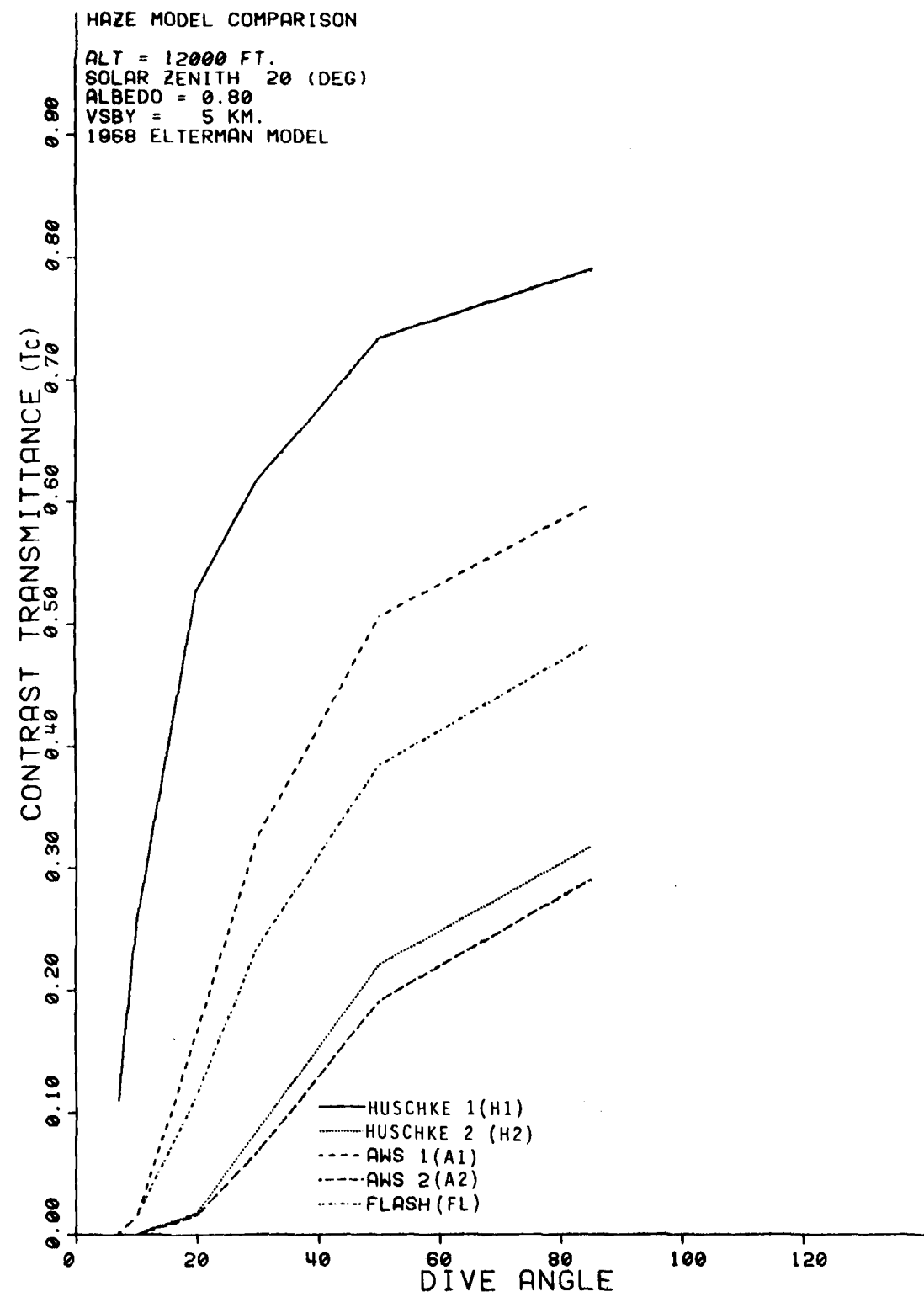


Figure 21. Contrast Transmittance at 20 Degrees Solar Zenith, Albedo of 0.80, and 5-km Surface Visibility.

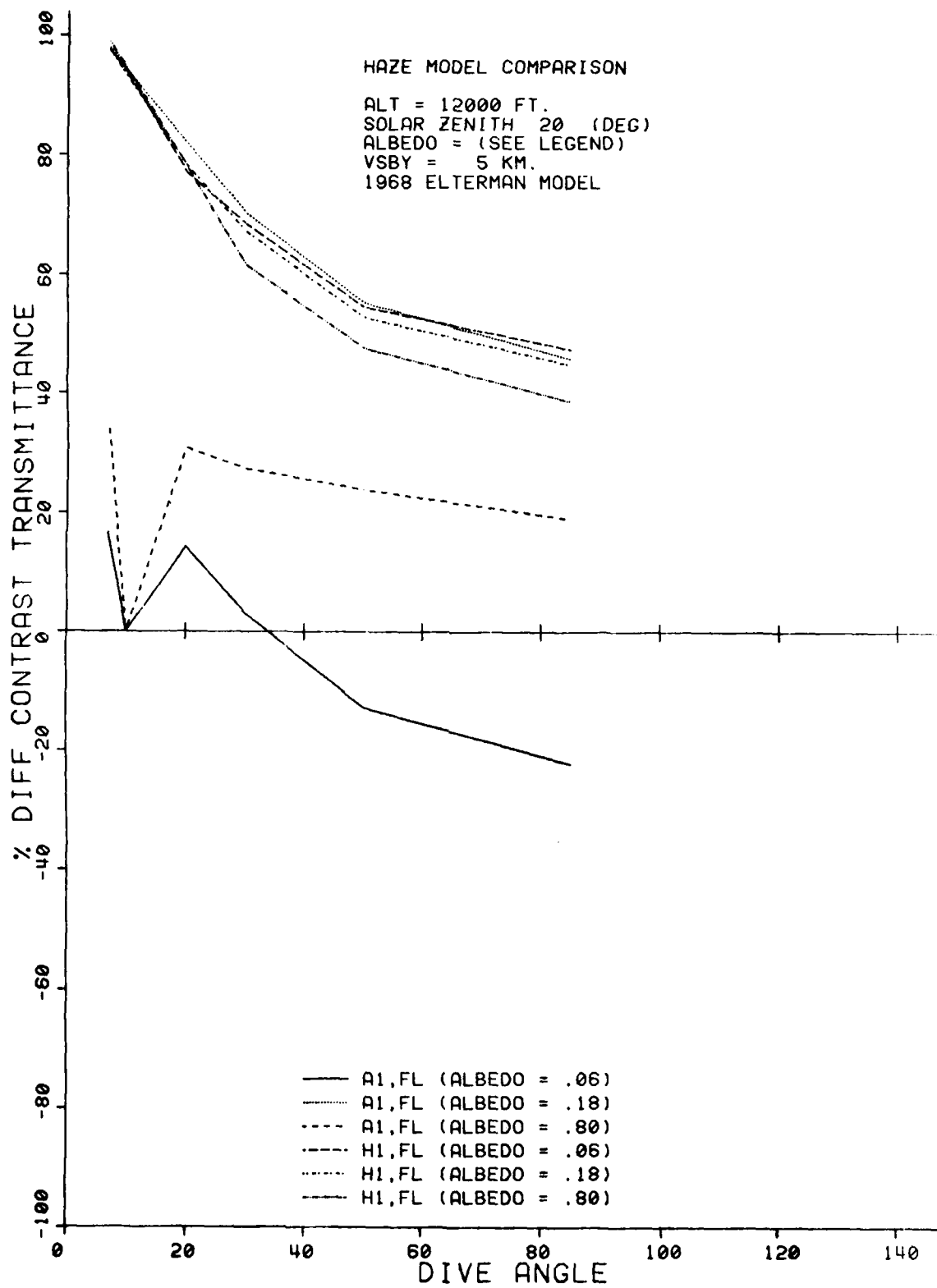


Figure 22. Model Comparisons at 20 Degrees Solar Zenith and 5-km Surface Visibility.

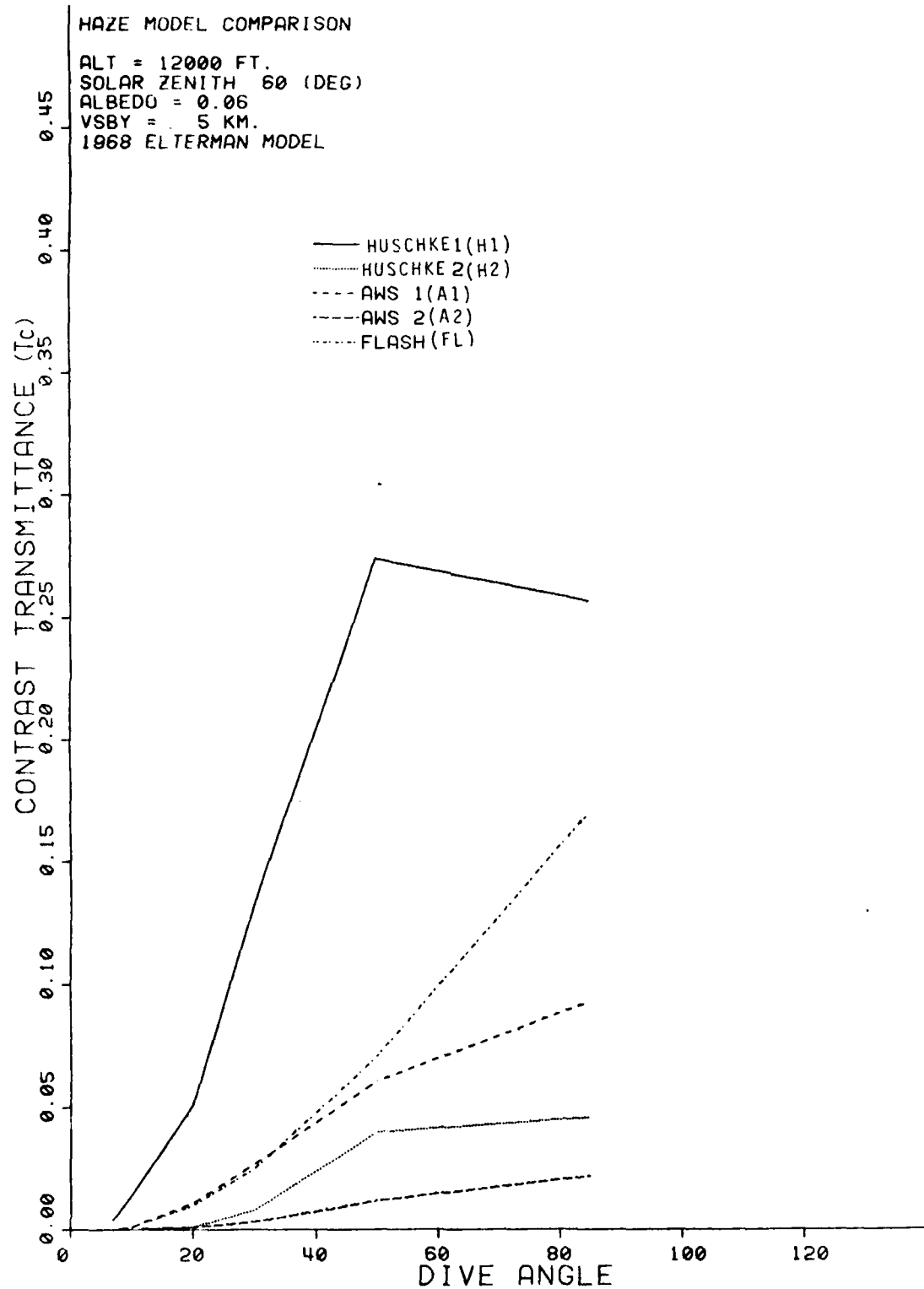


Figure 23. Contrast Transmittance at 60 Degrees Solar Zenith, Albedo of 0.06, and 5-km Surface Visibility.

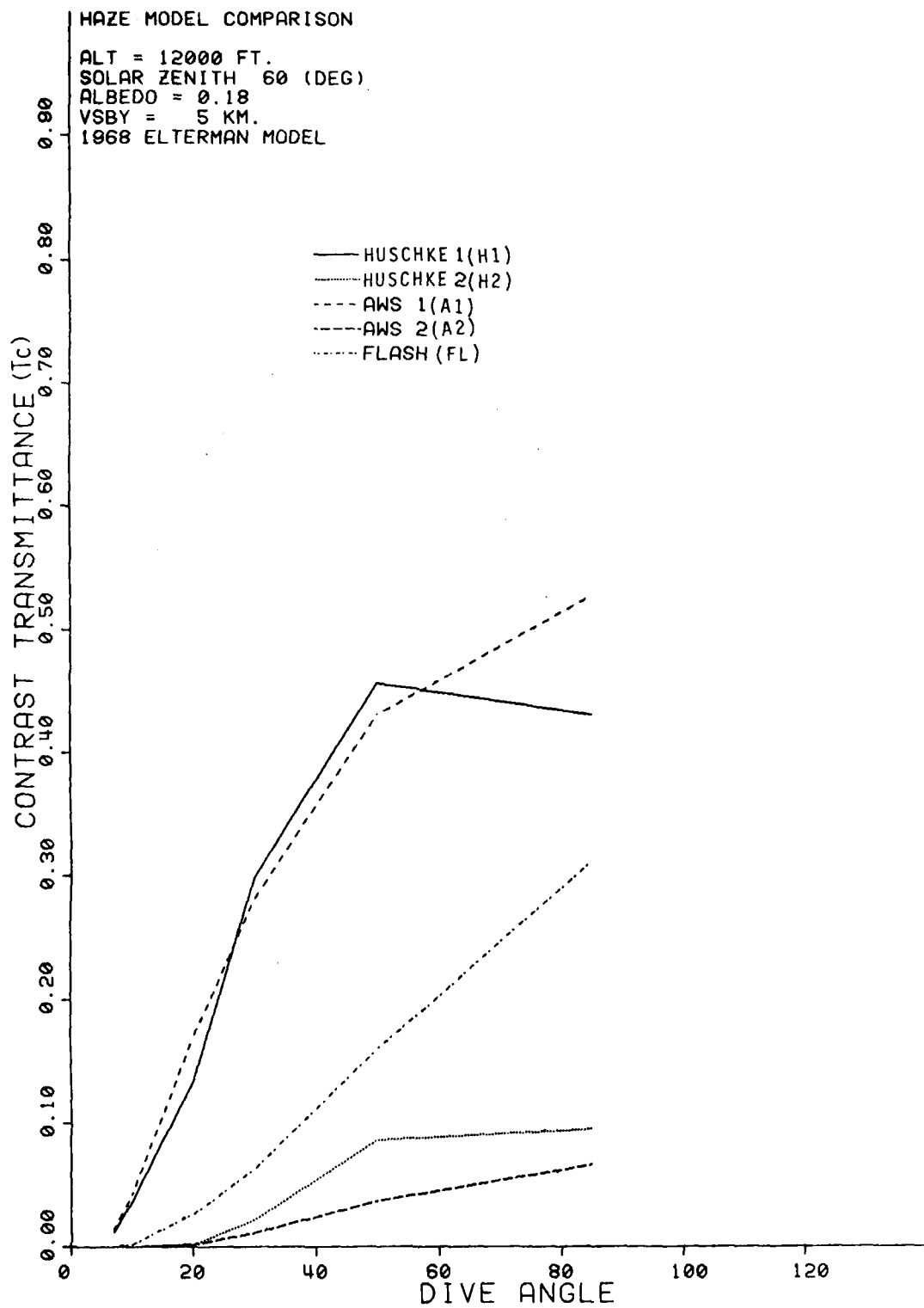


Figure 24. Contrast Transmittance at 60 Degrees Zolar Zenith, Albedo of 0.18, and 5-km Surface Visibility.

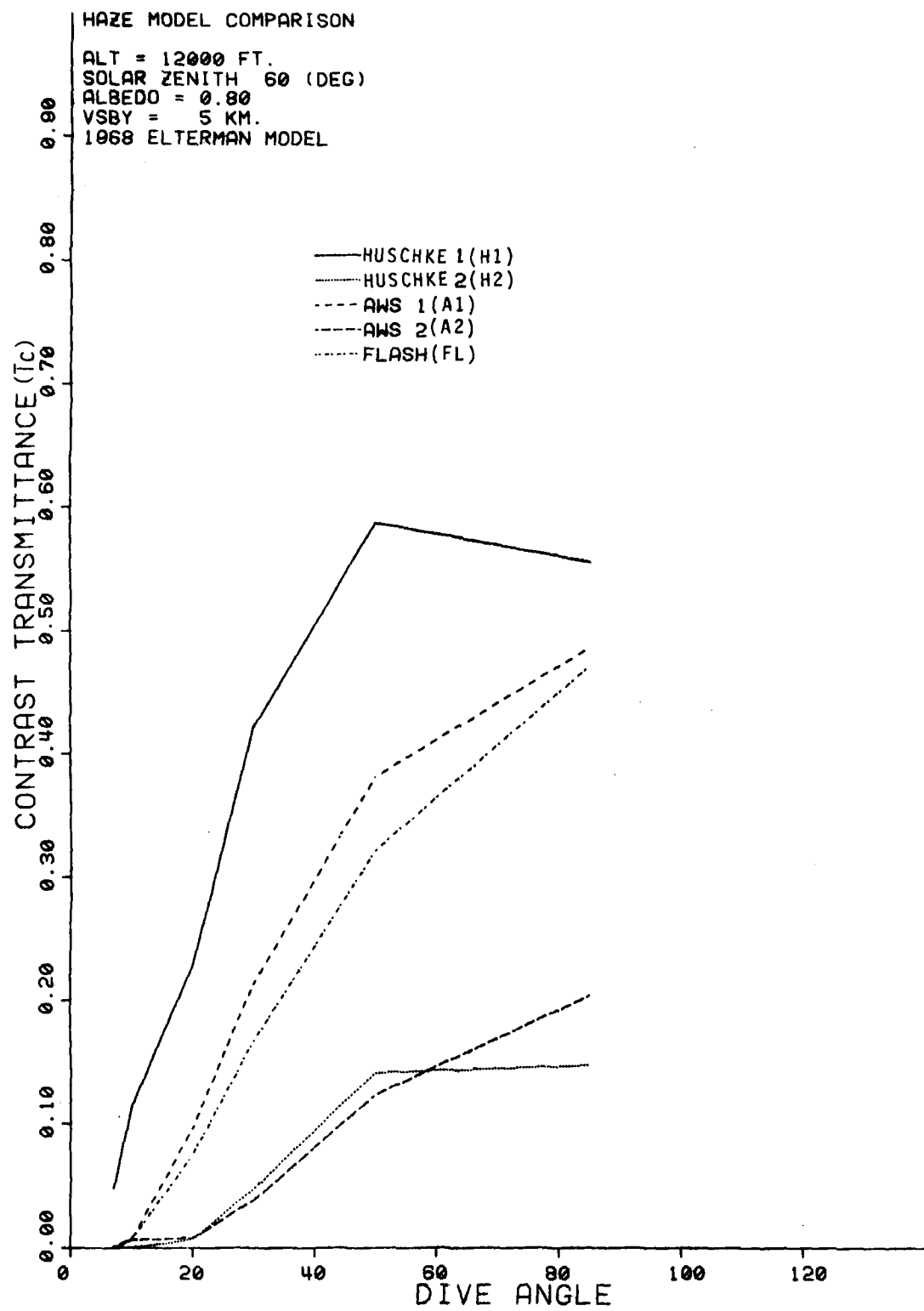


Figure 25. Contrast Transmittance at 60 Degrees Solar Zenith, Albedo of 0.80, and 5-km Surface Visibility.

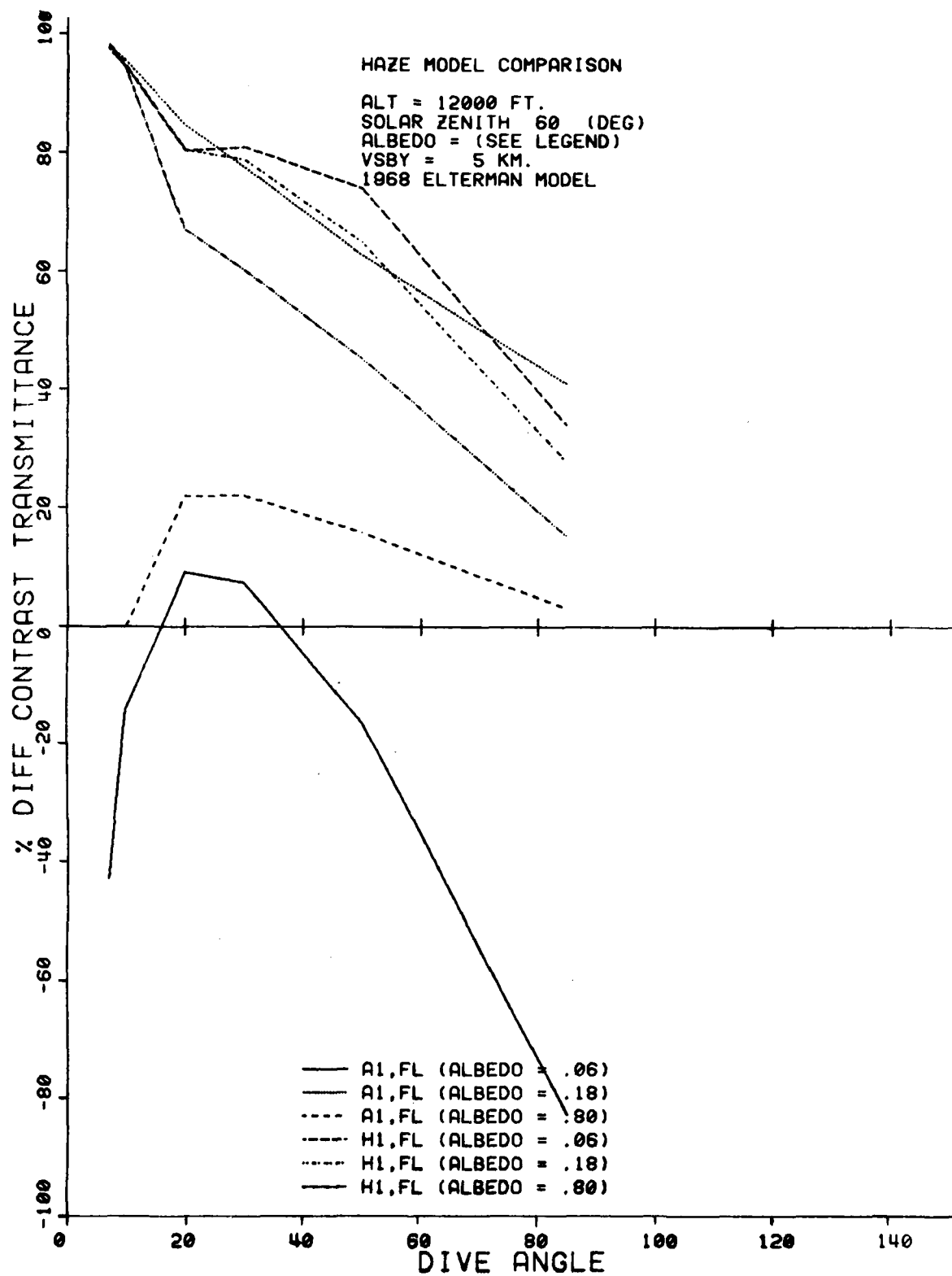


Figure 26. Model Comparisons at 60 Degrees Solar Zenith and 5-km Surface Visibility.

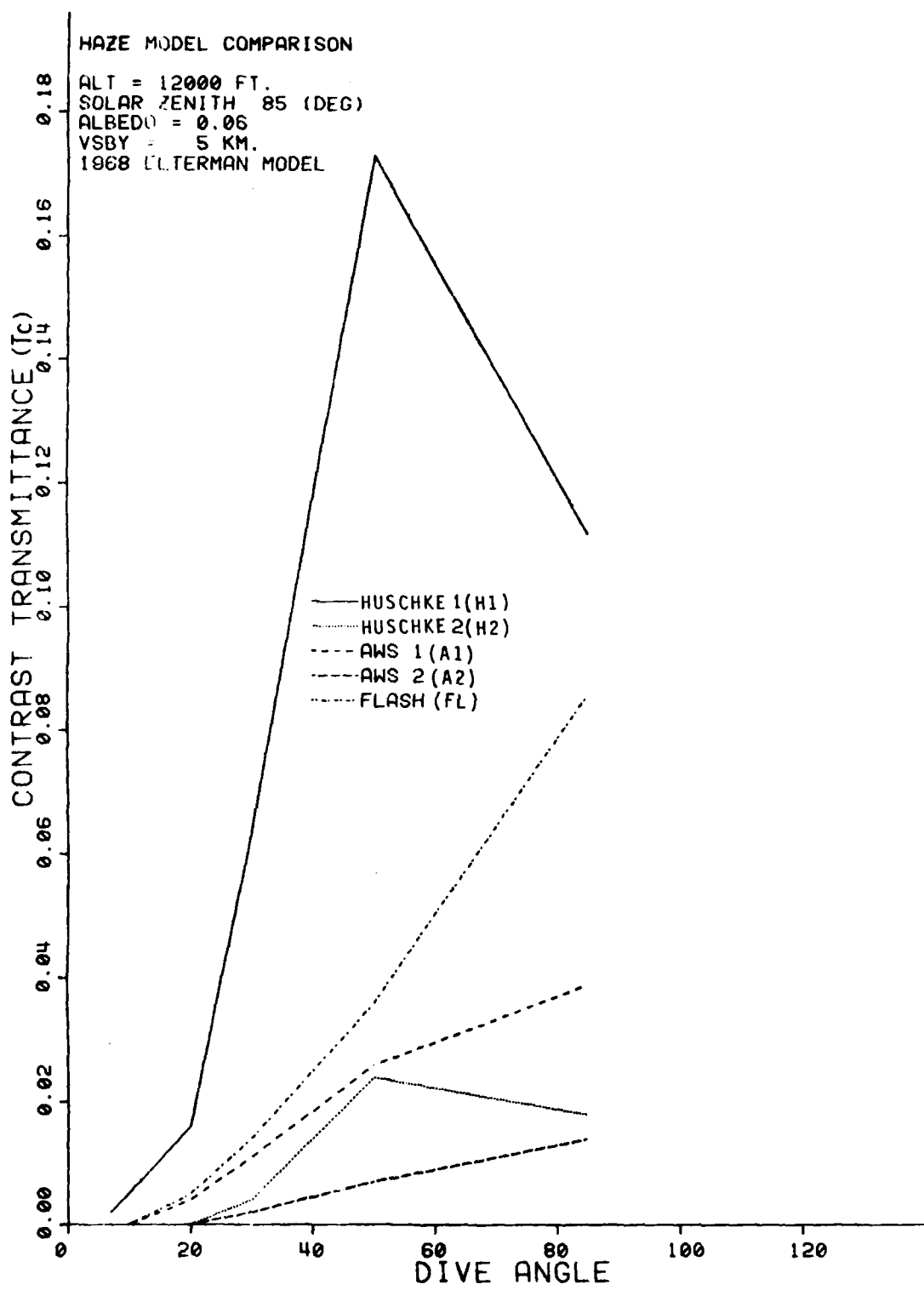


Figure 27. Contrast Transmittance at 85 Degrees Solar Zenith, Albedo of 0.06, and 5-km Surface Visibility.

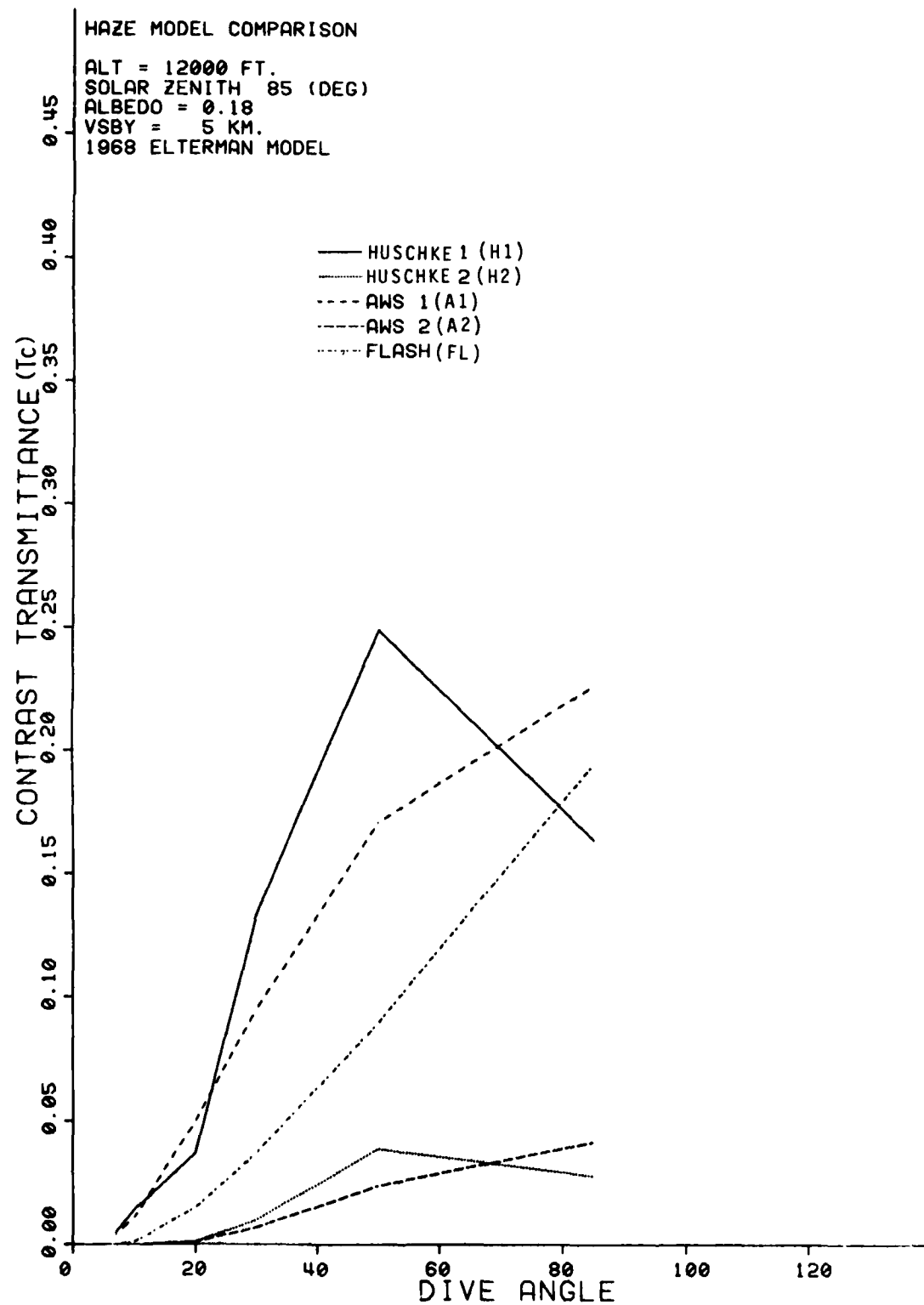


Figure 28. Contrast Transmittance at 85 Degrees Solar Zenith, Albedo of 0.18, and 5-km Surface Visibility.

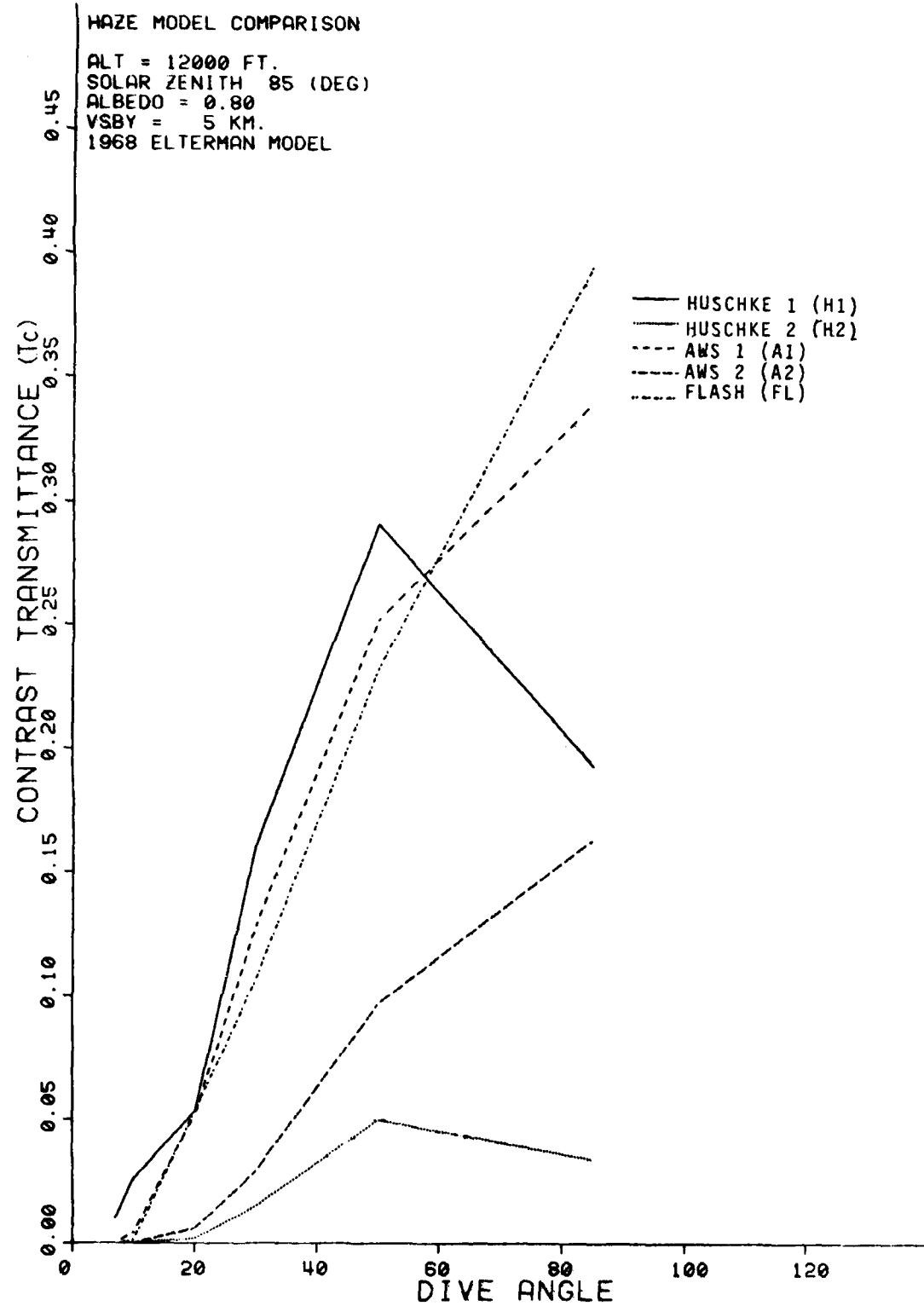


Figure 29. Contrast Transmittance at 85 Degrees Solar Zenith, Albedo of 0.80, and 5-km Surface Visibility.

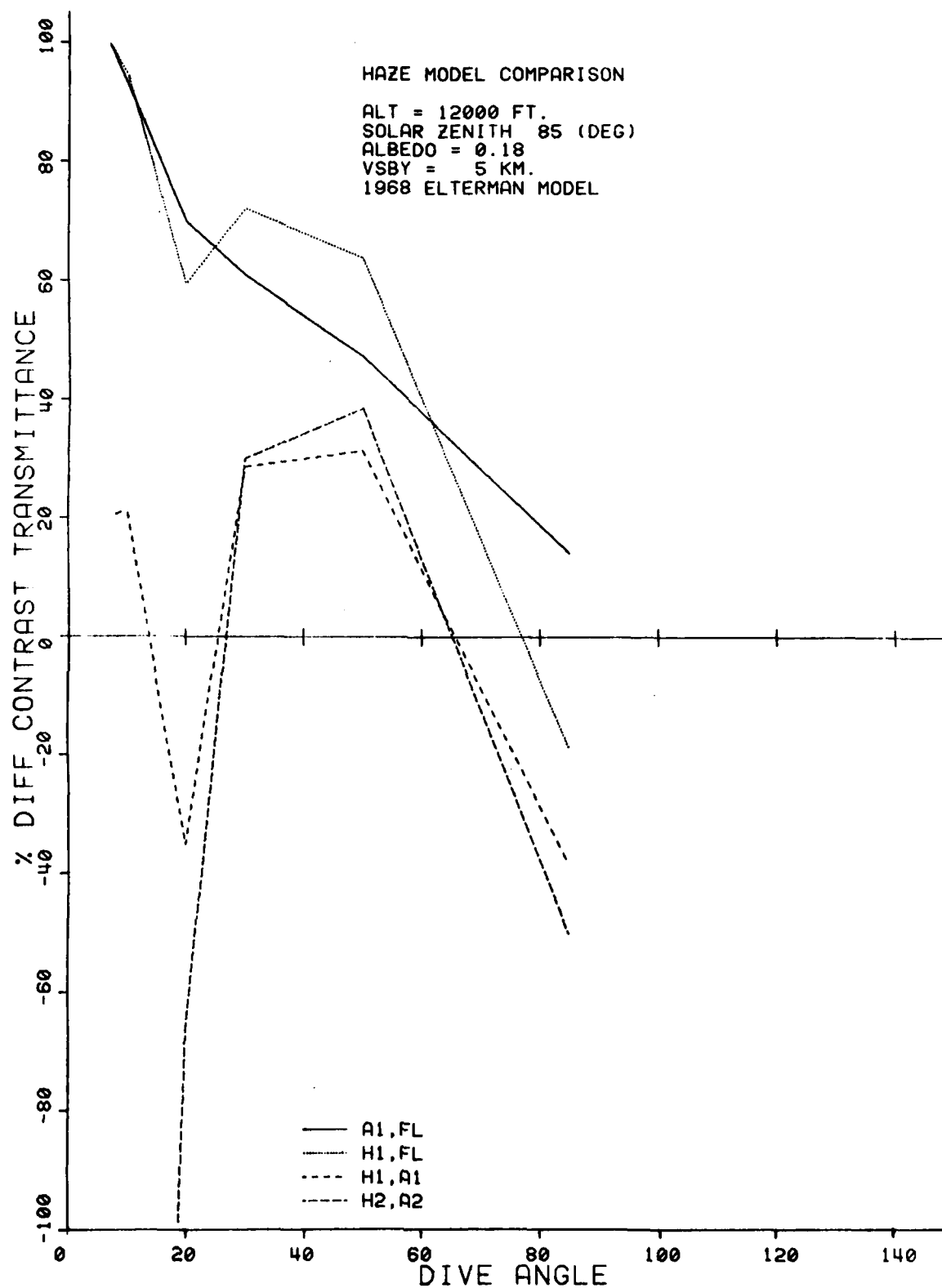


Figure 30. Model Comparisons at 85 Degrees Solar Zenith, Albedo of 0.18, and 5-km Surface Visibility.

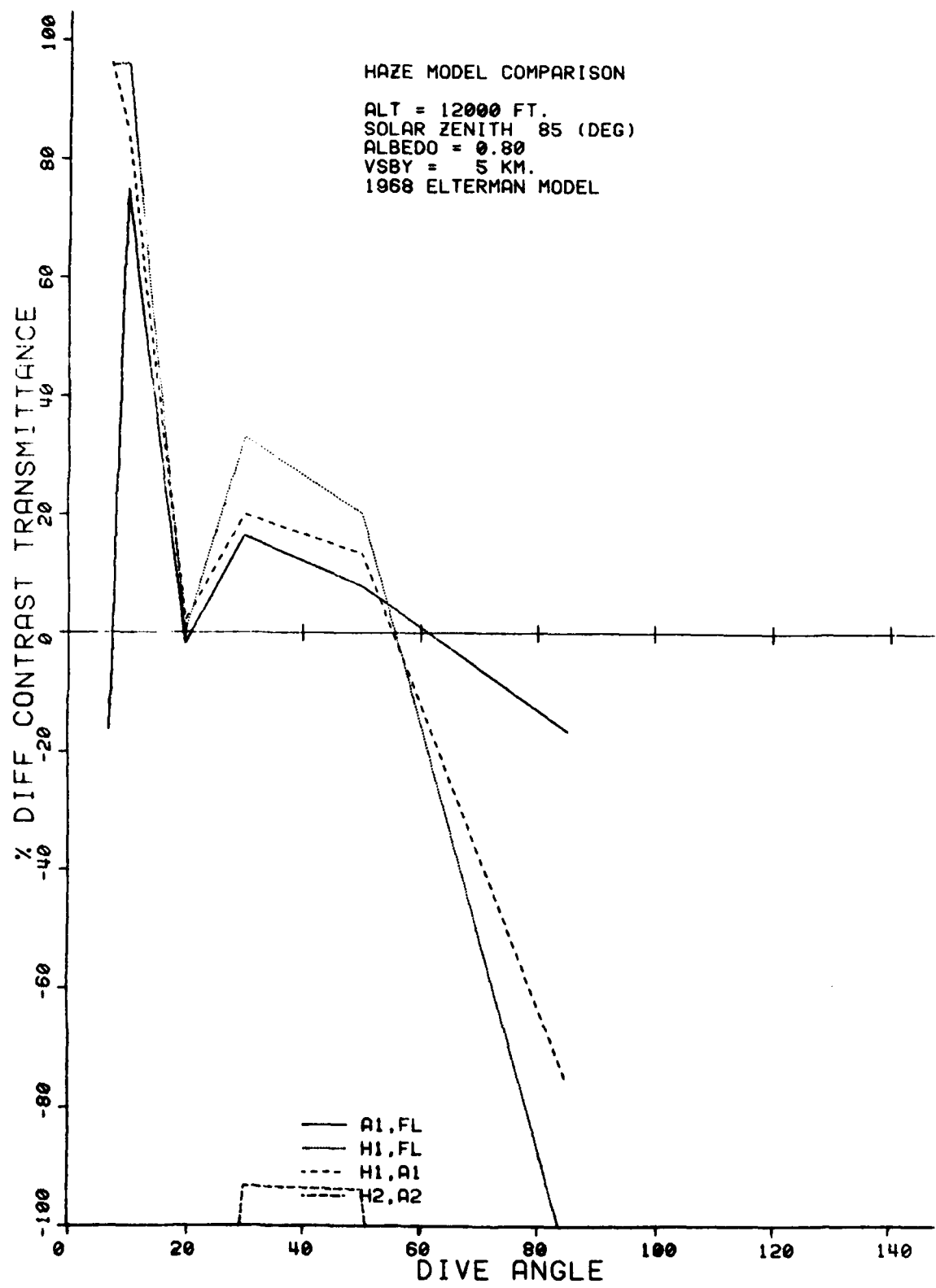


Figure 31. Model Comparisons at 85 Degrees Solar Zenith, Albedo of 0.80, and 5-km Surface Visibility.

less variability than Huschke. Also, for these sun and dive angles, the AWS 1500-meter mixing layer stair-step model (A2) does not compare favorably with the Huschke 1500-meter model (H2). Both do badly when compared to FLASH.

Figure 32, which shows the mean of the squared differences (RMSE) in T_c values for all dive angles indicates that, overall, the Huschke model compares well with the AWS model at all sun angles although neither is particularly good when compared with FLASH.

In summary, a comparison of the output from the Huschke and AWS models with that from FLASH with similar input reveals that, for a visibility of 5 km, neither model is without fault if FLASH is assumed to be ground truth. The Huschke model is either overly optimistic or overly pessimistic, depending on which mixing depth is used, and the AWS model output is highly variable, depending on which background albedo is used. In general, both the Huschke H1 and AWS A1 models tend to predict much larger values which are double those for FL in some cases. Both H2 and A2 routinely predict smaller values than FL.

Figure 33 compares the values of the total optical depth (0.55 microns) below the viewing altitude for the Huschke (stair-step) versus the FLASH, DART, and AWS A1 models (exponential). Note that the total optical depth for the exponential models (0.780) lies about midway between that for the Huschke 200-meter model (0.325) and the Huschke 1500-meter model (1.28). As the mixing depth increases above 200 meters, the total optical depth increases until it equals that for the exponential models near a mixing depth of 800 meters. One would thus expect that H1 would predict much smaller T_c values (vice FLASH, DART, AWS A1) and that H2 would predict much larger values than these three models.

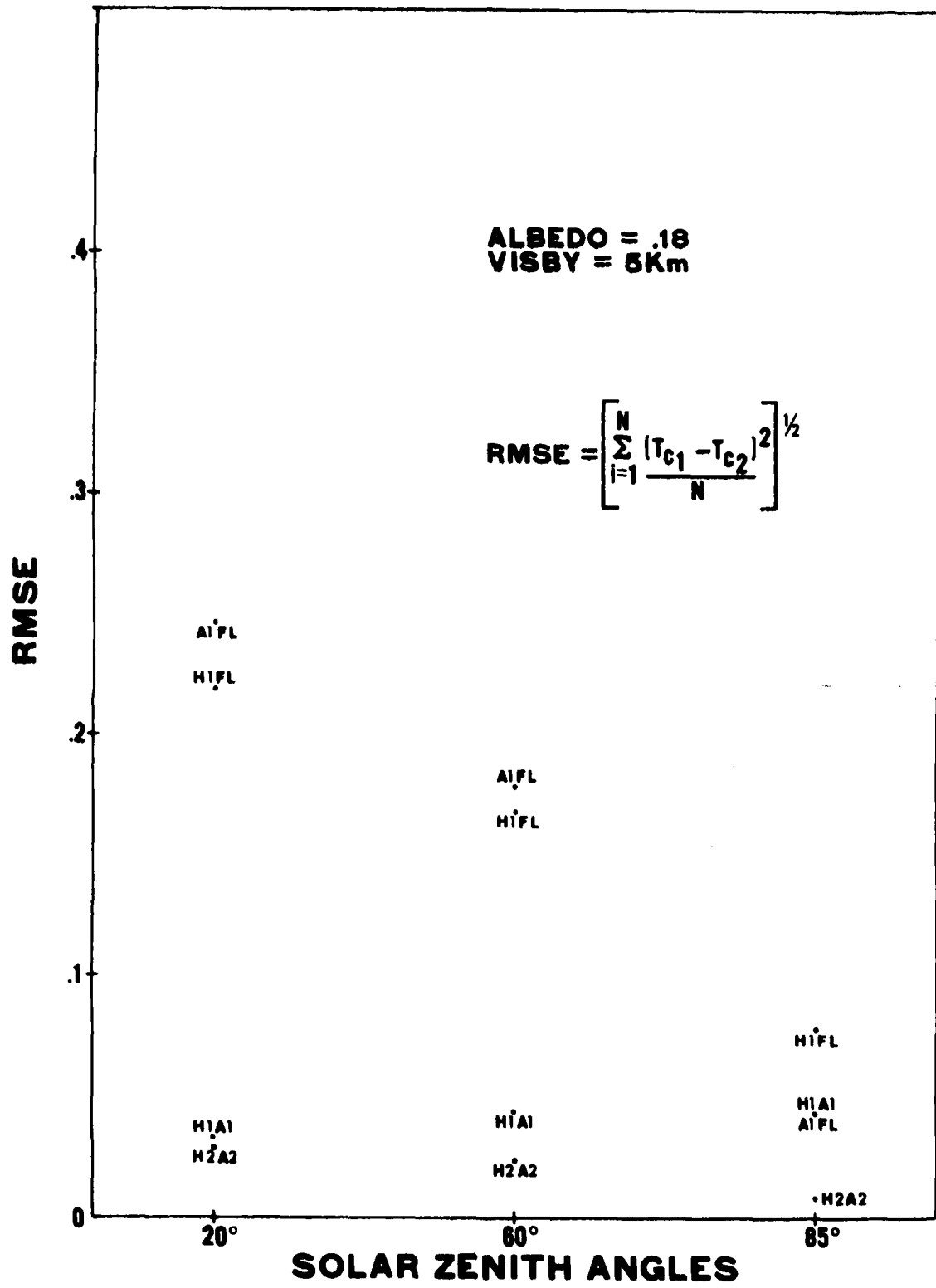


Figure 32. RMSE Model Comparisons for Albedo of 0.18 and 5-km Surface Visibility.

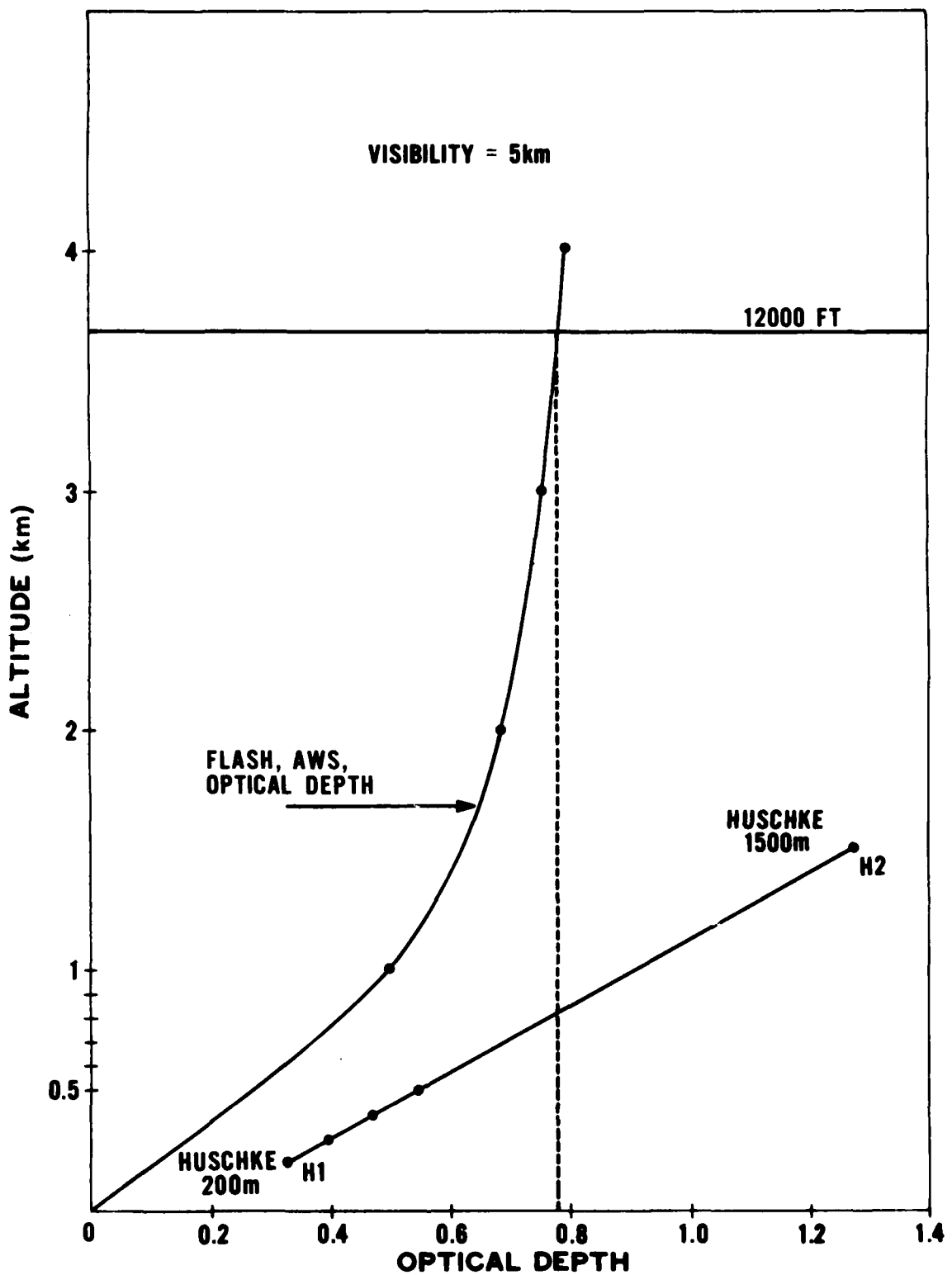


Figure 33. Total Optical Depth Below 12,000-Ft Viewing Altitude for 5-km Surface Visibility.

Chapter 5

CONCLUSIONS AND RECOMMENDATIONS

Conclusions

As mentioned previously at the end of Chapters 3 and 4, the Huschke and AWS models do a fairly acceptable job of duplicating FLASH contrast transmittance values when the surface visibility is good (23 km), but show larger deviations from FLASH as the visibility decreases to 5 km. Some of these deviations can be attributed to differences in the total optical depth below the sensor, i.e., differences between exponentially decreasing and stair-step extinction coefficient profiles. A less significant portion may be due to the fact that the Huschke model contrast transmittance values are independent of the sun-target-sensor azimuthal angle. If one computes Huschke T_c values for mixing depths at which the exponential and stair-step profiles optical depths are equal (425 meters for 23 km and 800 meters for 5 km) the Huschke values are closer to the FLASH values than those computed previously for mixing depths of 200 meters or 1500 meters. In some cases, the T_c values now fall within the range of FLASH T_c for 0° , 90° , and 180° azimuthal angles.

The importance of being able to predict the mixing depth and surface visibility with a fair degree of accuracy in the support of PGM operations cannot be overemphasized. Even perfect predictions of these two variables, used as input to the Huschke or AWS model, would still not result in perfect predictions of slant path contrast transmittance (assuming FLASH is ground truth). When one further considers that predictions of mixing depth and visibility are relatively new and of uncertain accuracy, the selection of a model to support TV-guided PGM operations becomes more complex. Clearly, a supposedly exact radiative transfer model (FLASH) with imperfect input data will produce contrast transmittance data of diminished usefulness to the tactical decision maker. On the other hand, an approximate model (Huschke, AWS) will produce data that may be less exact, but at a large reduction in computer processing time. The price one pays for using a more sophisticated model to support PGMs may therefore be ill-advised, since the three most important input variables (mixing depth, visibility, albedo) are based on still unproven forecasting techniques. Therefore, for the reasons listed above, a simple model such as Huschke's appears to meet the criteria of being "good enough" to support TV-guided PGM operations.

Recommendations

Based on the results of this study and the arguments presented above, USAFETAC makes the following recommendations relative to the selection of a model to support TV-guided PGMs:

- a. That the Huschke model be modified for dive angles greater than 82° to produce values of contrast transmittance that more nearly approximate the FLASH predictions.
- b. That this modified Huschke model be adopted by AWS as the standard model for both field and centralized facility support to TV-guided PGM operations.
- c. That AWS units employing the Huschke model undertake an ongoing evaluation to improve the overall capabilities of the model.

REFERENCES

Breitling, P.J. and Pilipowskyj, S., 1970: Computer Simulation of Optical Contract Reduction Caused by Atmospheric Aerosol. AIAA Paper No. 70-194, January 1970.

Collins, D.C. and Blattner, W., 1970: Utilization Instructions for Operations of the FLASH Monte Carlo Procedure on the AFCRL CDC-6600 Computer. Research Note RRA-N7023, 30 September 1970.

Cottrell, K.G., et al., 1979: Weather Support for Precision Guided Missiles, Electro-Optical Handbook, Vol I. AWS/TR-79/002, May 1979 (AD-A075168).

Duff, E.A., 1972: Atmospheric Contrast Transmission: Application to the Electro-Optical Lock-on Problem. Masters Thesis, AFIT, Wright-Patterson AFB, Ohio, June 1972.

Elterman, L., 1968: UV, Visible, and IR Attenuation for Altitudes to 50 Km, 1968. AFCRL Environmental Research Papers No. 285, AFCRL-68-0153, April 1968.

Elterman L., 1970: Vertical Attenuation Model with Eight Surface Meteorological Ranges 2 to 13 Kilometers. Tech. Report AFCRL-70-0200, March 1970.

Huschke, R.E., 1976: Atmospheric Visual and Infrared Transmission Deduced from Surface Weather Observations: Weather and Warplanes VI. R-2016-PR, October 1976.

Whitney, C.K. and Malchow, H.L., 1977: Study of Radiative Transfer in Scattering Atmospheres. C.S. Draper Laboratory Inc., Final Report under Contract No. F 19618-76-C-0223, June 1977.

5th Weather Wing, 1977: TV Maverick Missile (AGM-65A) Manual Weather Support Procedures. 23 February 1977.

GLOSSARY

AF	Air Force
AFGL	Air Force Geophysics Laboratory
AGL	above ground level
AWS	Air Weather Service
A1	AWS haze model with exponential profile
A2	stair-step extinction coefficient profile with mixing depth of 1500 meters
DART	Draper Lab's radiative transfer model
DT	Draper Lab's DART model
EO	Electro-Optical
EOGB	Electro-Optical Guided Bomb
FL	results of FLASH Monte Carlo model
FLASH	AFGL radiative transfer model
H1	output from Huschke model and mixing depth of 200 meters
H2	output from Huschke model and mixing depth of 1500 meters
LGB	Laser Guided Bomb
PGM	Precision Guided Munitions
SWG	Systems Working Group
T _C	contrast transmittance
USAFETAC	US Air Force Environmental Technical Applications Center
WSP	Weather Support Plan
SWW	5th Weather Wing

DISTRIBUTION LIST
USAFETAC/TN-82/001

HQ USAF(XOOTF)	1
HQ MAC(HO, PAL)	2
HQ AWS(DN, DNT)	3
Det 1	1
Det 2	1
Det 3	1
Det 6	1
OL-B	1
OL-I	1
OL-K	1
2WS(DO, DOU)	2
ASD/WE	1
AFWL/WE	1
Det 10	1
Det 11	1
Det 21	1
Det 30	1
1WW/DN	1
30WS	1
2WW/DN	1
7WS	1
28WS	1
31WS	1
3WW/DN	1
9WS/DON	1
11WS/DN	1
12WS/DN	1
26/WS	1
5WW/DN	1
1WS	1
3WS	1
5WS	1
6WS	1
24WS	1
25WS	1
7WW/DO	1
15WS	1
17WS/DON	1
3350/TCHTG/TTGW-W	1
AFGWC(DAPL, DO, TS, WF)	4
USAFETAC(DAJ, DN, DNA,	
TS, TSK)	5
Special Distribution	131
AWSTL Stock	<u>42</u>
Total Printed	225

